Biochimica et Biophysica Acta 1827 (2013) 1362–1377

Contents lists available at ScienceDirect

Biochimica et Biophysica Acta

journal homepage: www.elsevier.com/locate/bbabio

Review

The mechanism of ubihydroquinone oxidation at the Q_o-site of the cytochrome bc_1 complex☆

Antony R. Crofts [a,b,*], Sangjin Hong [b], Charles Wilson [a], Rodney Burton [b], Doreen Victoria [b], Chris Harrison [c,d], Klaus Schulten [a,c,d]

[a] Center for Biophysics and Computational Biology, University of Illinois, Urbana, IL 61801, USA
[b] Department of Biochemistry, University of Illinois, Urbana, IL 61801, USA
[c] Department of Physics, University of Illinois, Urbana, IL 61801, USA
[d] Theoretical Biophysics Group, Beckman Institute, University of Illinois, Urbana, IL 61801, USA

ARTICLE INFO

Article history:
Received 10 August 2012
Received in revised form 12 December 2012
Accepted 18 January 2013
Available online 8 February 2013

Keywords:
Bifurcated reaction of Q-cycle
Control and gating
Semiquinone occupancy
H^+ exit pathway
Kinetic model

ABSTRACT

1. Recent results suggest that the major flux is carried by a monomeric function, not by an intermonomer electron flow. 2. The bifurcated reaction at the Q_o-site involves sequential partial processes, — a rate limiting first electron transfer generating a semiquinone (SQ) intermediate, and a rapid second electron transfer in which the SQ is oxidized by the low potential chain. 3. The rate constant for the first step in a strongly endergonic, proton-first-then-electron mechanism, is given by a Marcus–Brønsted treatment in which a rapid electron transfer is convoluted with a weak occupancy of the proton configuration needed for electron transfer. 4. A rapid second electron transfer pulls the overall reaction over. Mutation of Glu-295 of cyt *b* shows it to be a key player. 5. In more crippled mutants, electron transfer is severely inhibited and the bell-shaped pH dependence of wildtype is replaced by a dependence on a single p*K* at ~8.5 favoring electron transfer. Loss of a p*K* ~6.5 is explained by a change in the rate limiting step from the first to the second electron transfer; the p*K* ~8.5 may reflect dissociation of QH•. 6. A rate constant ($<10^3$ s^{-1}) for oxidation of SQ in the distal domain by heme b_L has been determined, which precludes mechanisms for normal flux in which SQ is constrained there. 7. Glu-295 catalyzes proton exit through H^+ transfer from QH•, and rotational displacement to deliver the H^+ to exit channel(s). This opens a volume into which $Q^{\bullet -}$ can move closer to the heme to speed electron transfer. 8. A kinetic model accounts well for the observations, but leaves open the question of gating mechanisms. For the first step we suggest a molecular "escapement"; for the second a molecular ballet choreographed through coulombic interactions. This article is part of a Special Issue entitled: Respiratory complex III and related bc complexes.

1. Introduction

In the Q-cycle mechanism of the bc_1 complex (Fig. 1), oxidation of QH_2 at the Q_o-site occurs through a bifurcated reaction delivering the electrons to two different acceptor chains [1–4]. The first electron reduces the high potential chain (ISP and cyt c_1), and generates an intermediate semiquinone (SQ_o) in QH• form. The electron from SQ_o reduces the low potential chain, consisting of hemes b_L and b_H of cyt *b*, which deliver the electron across the membrane to reduce ubiquinone (Q) or SQ_i at the Q_i-site in an electrogenic process that contributes to the electrical component of the proton gradient used to drive ATP synthesis. Mitchell's original Q-cycle involved a co-participation of dehydrogenases, but Garland et al. [5] pointed out that the isolated complex functions as a standard-alone enzyme, and suggested a modified Q-cycle, which was included among several variants reviewed by Mitchell in 1976 [1]. This modified Q-cycle was shown to best explain the behavior of the complex in photosynthetic bacteria [2] (see [3] for a historical perspective). Structures of increasingly detailed resolution have become available over the last dozen years for both mitochondrial and bacterial complexes, and these have revealed dynamic processes [6], and allowed refinement of understanding to the molecular level. Kinetic and thermodynamic studies of mutant strains modified at key residues have allowed dissection of critical reactions into partial processes, and definition of their physicochemical parameters (cf. [7–13]). The consensus version of the Q-cycle has depended for much of its detail on work from photosynthetic bacteria, and this had allowed us to develop a mechanistic model that accounted well for known features of the

Abbreviations: SQ, semiquinone (dissociation state unspecified); QH•, neutral semiquinone; $Q^{\bullet -}$, anionic semiquinone; QH_2, ubihydroquinone-10, ubiquinol, quinol; Q, ubiquinone-10, quinone; ISP, Iron–sulfur protein; SU IV, subunit IV; ROS, reactive oxygen species; ES_1, ES_2, enzyme–substrate complexes for first and second electron transfers, respectively

☆ This article is part of a Special Issue entitled: Respiratory complex III and related bc complexes.

* Corresponding author at: Department of Biochemistry, 419 Roger Adams Lab, 600 S. Mathews Ave, Urbana, IL 61801, USA. Tel.: +1 217 333 2043; fax: +1 217 244 6615.
E-mail address: crofts@illinois.edu (A.R. Crofts).

0005-2728/$ – see front matter © 2013 Elsevier B.V. All rights reserved.
http://dx.doi.org/10.1016/j.bbabio.2013.01.009

forward chemistry. The structure is dimeric, but most schematic representations of the Q-cycle show a monomeric complex, and the question of whether this implies a monomeric function is still not settled.

As a preliminary to addressing mechanistic questions, we must first deal with the question of whether the turnover of the complex involves a monomeric or dimeric mechanism for its main flux.

2. Monomeric or dimeric function

In a previous review [9] we had asked the question of how well a monomeric Q-cycle mechanism could account for the function of the dimeric bc_1 complex. The answer we favored, which could be paraphrased as "pretty well", has been challenged by most other groups working in this field [8,14–24]. The alternative scenarios suggested have offered a variety of mechanisms in which electron transfer across the dimer interface was important in normal forward chemistry, and in several cases, carried the full flux of turnover. To a greater or lesser extent, these alternative mechanisms would require re-evaluation of the data that had led to identification in the 1980s of Garland's modified Q-cycle [2,5,25–29] as the most economical hypothesis. Rather than repeating the detailed arguments in the previous review, we will focus on developments that since then have been claimed to demonstrate that intermonomer electron transfer occurs at rates compatible with an important role in normal flux [14,16,19,30–32]. Does the proposed intermonomer electron transfer represent a challenge demanding a paradigmatic change in our thinking, or a diversion?

In each of three earlier papers [14,16,19], the strategy was to use molecular engineering in bacterial systems to set up a protocol in which a heterodimeric bc_1 complex could be expressed. Then, differential mutation in two copies of the gene encoding cyt *b* was carried out, such that either could carry a crippling mutation for monomeric function. Intermonomer transfer could then be tested in a heterodimer enforcing turnover by electron transfer across the dimer interface at the level of heme b_L. The difference in strategies between the three labs was in how the heterodimeric system was implemented. In two of the groups [14,16], two separate copies of the gene encoding cyt *b* were introduced using two plasmids, each with a distinctive tag to facilitate isolation of heterodimeric complexes containing both tags by sequential affinity chromatography. The disadvantage of this approach is that the bacteria then generate in situ a mixed population of bc_1 complexes, only half of which carry the function designed. This leads to difficulties in the interpretation of experiments in which function is tested in the native membrane, and the need for more detailed work using the isolated protein. The Osyczka group [19] introduced a neat way to overcome this problem. In their construct, a one plasmid system, the two copies of the gene encoding cyt *b* were joined by in-frame sequence for a protein linker span so as to express a linked heterodimeric cyt *b* of twice the size as the monomeric version. Then all copies of the dimeric complex might be expected to have the same pair of linked cyt *b* subunits, which could nevertheless be differentially mutated to produce similar vehicles for testing intermonomer function.

The experimental results from these three studies seemed unequivocal.

In Castellani et al. [14], the heterodimeric constructs were designed for expression in *Paracoccus denitrificans* so as to enforce a half-of-sites functionality, and stopped-flow kinetic measurements on the isolated heterodimeric complexes then showed essentially the same monotonic kinetics of reduction of heme b_H as observed in wildtype, and the same difference in amplitude, a 1:0.5 ratio between the heme b_H and heme c_1 reduction, claimed to be diagnostic of such a functionality. In order to account for these characteristics in the half-of-sites mechanism, it is necessary to postulate that intermonomer electron transfer occurs with an intrinsic rate substantially faster than the rate limiting step, since otherwise a biphasic reduction of heme b_H would have been seen.

In Świerczek et al. [19], using the single plasmid approach and a linked heterodimer expressed in *Rhodobacter capsulatus*, one copy of cyt *b* was blocked by mutation G158W, disabling the Q_o-site, and the other by mutation H212N of a heme b_H ligand, disabling binding and blocking electron transfer in the low-potential chain. For the critical strain, $_W$B-B^N carrying both mutations, the kinetics of heme b_H reduction were complete in ~5 ms, suggesting a half-time <2 ms, in the same range as the wildtype ~1 ms. Similarly, kinetics of cyt *c* re-reduction and steady-state rates were "…never less than half…" those in wildtype. These seemed to support the claim of the title, "…An electronic bus bar lies in the core of cytochrome bc_1…".

In Lanciano et al. [16], also working with *Rb. capsulatus*, the claim was more modest, that intermonomer electron transfer was sufficient to support anaerobic photosynthetic growth (which requires a functional bc_1 complex). Mutations similar to those in [19] were introduced in the two plasmid system, and as in [19], the heterodimeric constructs enforcing intermonomer electron transfer showed kinetics of heme b_H reduction and bc_1 turnover in the low ms range, suggesting rapid flux through this pathway.

In our own attempts to express in *Rhodopseudomonas sphaeroides* [33] a system similar to that in [19], we believed initially that we had confirmed the previous data; strains harboring suitable constructs to enforce intermonomer function showed essentially the same kinetics as those of the wildtype. This was somewhat surprising because linear inhibitor titrations, and the poise of reactants following activation by one or two flashes at different points in the titration, were not compatible with such a flux. However, careful examination of the DNA sequences supporting this behavior revealed that all active colonies had reconstructed the wildtype monomeric operon by crossover recombination using the unmodified spans from the two copies originally introduced. The only survivors on growth under photosynthetic conditions (requiring an active bc_1 complex) were either these reconstructed homodimeric wildtype strains, or heterodimeric strains in which at least one monomer catalyzed a functional Q-cycle. We concluded that on growth under photosynthetic conditions, intermonomer electron transfer could not compete for survival with monomeric function. Examination of the earlier papers showed little or no recognition that similar genetic mechanisms might have played a part [14,16,19]. However, subsequent reports from two of the groups showed that they had been fully aware of the problem, had taken serious steps to mitigate it, and that their results were obtained on preparations that had to be grown under non-photosynthetic conditions to avoid selection of homodimeric reconstructs [31,32]. In a more recent report, it had proved possible in the one-plasmid system to isolate from strains grown under aerobic conditions (in which an active bc_1 complex is not required), and to purify heterodimeric complexes in which activity could be tested [30]. Complexes with one functional monomer showed about half the activity of complexes in which both monomers were functional. Those complexes designed to enforce inter-monomer electron transfer showed much lower activity; the authors claimed ~17% that of fully active complexes, but their data indicate that most of this activity was independent of substrate [cyt *c*], so only a much lower value is defensible. These results were quite consistent with our own. The rapid kinetics claimed to show inter-monomer electron transfer in the earlier papers could not have been attributed to complexes showing this low activity, and it seems much more likely that they reflected the activity of wildtype reconstructs. Although the work in *P. denitrificans* has not been further discussed, the conditions for growth by respiration would have been highly selective for wildtype, and, without special precautions, it seems unlikely that cross-over recombination could have been avoided.

In this review, we will take the view that none of the claims for intermonomer electron transfer in the <2 ms range have been substantiated, and that the simple monomeric function remains the most reliable starting point for further discussion [33]. Intermonomer electron transfer may well occur, but not at a rate that represents any substantial

fraction of the normal forward flux. Some interesting possibilities for amelioration of damaging short-circuits by intermonomer flux have been discussed [34,35], but do not require rapid flux.

3. The Q_o-site reaction

Although the general mechanism is well understood (Fig. 1), there is little agreement as to how the bifurcated reaction is controlled. The question of control plays out in a feature of the Q-cycle of anthropocentric interest — our mitochondria are slowly killing us. The context is the free-radical theory of aging [36–39]; in most cells, the respiratory chain is the main culprit in generation of reactive oxygen species (ROS), and the Q_o-site of the bc_1 complex is responsible for a substantial fraction [40,41]. The ROS production likely reflects an evolution of the bifurcated reaction initially in an anaerobic world. When evolution "invented" oxygenic photosynthesis, the biosphere had to adapt to the new poison [34]. The SQ intermediate generated in the bifurcated reaction (SQ_o) has the right potential to reduce O_2 to superoxide anion (O^-_2), which leads to a cascade of ROS that damage DNA and protein. Although species that failed to adapt became extinct, in extant forms the bifurcated reaction necessarily still operates through a SQ intermediate, and all still have a residual problem; under conditions in which electrons back-up in the low potential chain (inhibition of the Q_i-site, back-pressure from the proton gradient, etc. [40,42]), ROS production is exacerbated, likely because SQ_o accumulates. Several such bypass reactions (also called short-circuits [43]) have been discussed [10,40,43], all of which decouple the bifurcated reaction (which is essential for the primary role in generating the proton gradient) by shunting electrons from SQ_o to the high potential chain, or to O_2 under aerobic conditions. Because mitochondria operate in an aerobic environment, the question of how evolution has modified the complex to minimize these deleterious bypass reactions has an immediate medical importance.

One of the evolutionary strategies for mitigation of ROS production has been to hone the mechanism at the Q_o-site so as to operate with minimal occupancy of the SQ_o. Over the past few years, our research has established a strong case for a mechanism that depends on two main features that minimize ROS production [10,44–48]: (i) an endergonic first electron transfer that keeps the occupancy of the SQ_o intermediate low; and (ii) a rapid removal of SQ_o in the second electron transfer, facilitated by movement of SQ in the Q_o-site closer to the acceptor heme b_L. These play out in the partial processes of the electron transfers (Sections 3.1–3.3), and in control of the reaction, to be discussed in Section 5.

In the following sections we will briefly review the evidence that has led us to our present understanding of the mechanism of the Q_o-site reaction. Building on the modified Q-cycle, new features of the hypothetical framework [49–54] were proposed shortly after the first complete structure [6] became available.

3.1. The first electron transfer

At saturating substrate concentrations, the first electron transfer is rate-limiting and occurs through a proton-coupled electron transfer. The reaction is endergonic [44,45,47,55–57], and the products are ISPH and QH•. Removal of a H^+ generates the anionic species, $Q^{\bullet -}$, which is retained in the Q_o-site volume [55]. When substrates QH_2 or ISP_{ox} were limiting, the rate also varied as expected from the controlling role for substrate concentration in the formation of the initial reaction complex for this step, the ES_1-complex (ES_1) (Eq. (1)). This state likely involves the formation of an H-bond between N_ε of His-152 of ISP_{ox} and a ring −OH of QH_2 [54]. The reaction from ES_1 occurs through a proton-first-then-electron sequence; the rate depends on the contribution of pK_{ox1} of ISP_{ox} to the Brønsted barrier [58], which determines the distribution of the proton along the H-bond. Both proton and electron are transferred through the H-bond, but the proton has to be in the weakly populated state adjacent to the N-atom before the electron can transfer. The electron transfer rate constant depends on the short distance and the driving force, with a contribution from $E_{m,ISP}$ to the latter that could be varied by mutation around the cluster of ISP [59,60]. The behavior is then well-described according to a Marcus–Brønsted relationship [44,52]:

$$\log_{10}k = 13 - \frac{\beta}{2.303}(R-3.6) - \gamma\frac{(\Delta G^{o}_{ET}+\lambda_{ET})^2}{\lambda_{ET}} - \left(pK_{QH_2} - pK_{ISP_{ox}}\right) \quad (7)$$

in which the observed rate constant represents a convolution between the rapid electron transfer expected from Marcus theory (middle term on the RHS) within the distance constraints from a Moser–Dutton treatment (left term), and the weak probability for the proton distribution (the term on the right).

The formation of ES_1 likely involves binding of two substrates, QH_2 and ISP_{ox}, stabilized through an H-bond between them. This direct interaction suggests that with one substrate held constant at saturating concentration, variation of the other would give Michaelis–Menten behavior [44,47,61], allowing calculation of relative binding coefficients for both substrates:

$$Eb_Hb_L \cdot ISP_{ox} \underset{K_{QH_2}}{\overset{QH_2}{\rightleftharpoons}} Eb_Hb_L \cdot QH_2 \cdot ISP_{ox}; K_{QH_2} = \exp\left\{\frac{zF}{RT}\Delta E_m^{(ES-free)}\right\} \quad (8)$$

$$Eb_Hb_L.QH_2 \underset{K_{ISP_{ox}}}{\overset{ISP_{ox}}{\rightleftharpoons}} Eb_Hb_L.QH_2.ISP_{ox}; K_{ISP_{ox}} = 10^{\left(pK_{ox1}-pK_{app}\right)}. \quad (9)$$

The concentration of QH_2 can be varied by redox titration of the Q-pool over the range of ambient redox potential, E_h, around the E_m, keeping pH constant (which keeps $[ISP_{ox,dissoc}]$ constant, see below). We determined that the difference ($\Delta E_m^{(ES-free)}$, on the RHS of Eq. (8) between E_m of the free Q-pool (E_m^{free} ~90 mV at pH 7), and the apparent E_m for the formation of ES_1 (E_m^{ES}) [44] was ~30 mV, suggesting that K_{QH_2} ~10.

The form of ISP_{ox} involved in ES_1 is that in which His-152 is dissociated, and the concentration of this form varies with pH [13,47,62]. The apparent pK, pK_{app}, which describes the rising portion of the bell-shaped Brandt–Okun [63] pH dependence, can be determined by varying the pH. The $[QH_2]$ can be kept constant by choice of E_h close to the value of E_m^{free} appropriate to the experimental pH, to maintain the Q/QH_2 poise close to the midpoint, where $[QH_2]$ is almost saturating. The difference between the pK_{app} estimated like this, with a value ~6.5, and pK_{ox1} ~7.6 (in wildtype) of the isolated ISP, must reflect $K_{ISP_{ox}}$ (RHS of Eq. (9)), which also has a value ~10 (Eq. (9)).

The similarity between these values strongly supports the conclusion that the result gives the binding constant for the formation of ES_1. With ISP mutant strains, pK_{app} varied in parallel with changes in pK_{ox1} [47,60], demonstrating a direct correlation between the pK values, and supporting the suggestion that the H-bond from QH_2 to His-152 of ISP_{ox} represents a major component of the binding free-energy.

Central to the above scenario are the physicochemical properties of the ISP. These have been studied in detail through mutagenesis [13,59,64,65], thermodynamic characterization [13,62], spectroscopic studies [66–68], crystallographic structures at atomic resolution [11,13], and detailed kinetic analysis [13,44,47,51]. Complementary work using NMR and specific isotopic labeling in *Thermus thermophilus* [69,70] has identified the group responsible for the low pK_{ox1} in ISP as the histidine equivalent to His-152 in *Rb. sphaeroides*, with the second histidine ligand to the cluster being associated with the higher pK_{ox2}.

The set of values derived from this body of work and the complementary studies in *T. thermophilus* provide a secure experimental basis for the mechanism proposed.

3.2. The second electron transfer

In a series of papers published shortly after the first complete structures became available [47,49,50,53,54,71], we proposed a mechanism that included a pathway for the second electron transfer and the accompanying proton exit. The structures showed a capacious Q_o-site in which different classes of inhibitors occupied different domains. In modeling ES_1, we had noted that Glu-295 (E295, in *Rb. sphaeroides* numbering) formed an H-bond with the –OH of the stigmatellin ring, and suggested that a similar bond might be formed with the second ring –OH of quinol. This glutamate is part of a highly conserved sequence (-PEWY-) that forms one side of the Q_o-site. Although the context was ES_1, the interest with respect to the second step would be in the spatial configuration and the role in the formation of the reaction complex from which the second electron was transferred, the ES_2-complex (ES_2). Since stigmatellin occupied the domain distal from heme b_L, and provided the model for ES_1, this complex would necessarily form in this distal domain, and the intermediate product would also be formed there. Because the first electron transfer is neutral, the SQ_o would initially be in the neutral form, QH•. The subsequent evolution of the second electron transfer process was suggested to involve separation of QH• from the intermediate product state (the complex between QH• and ISPH) to form

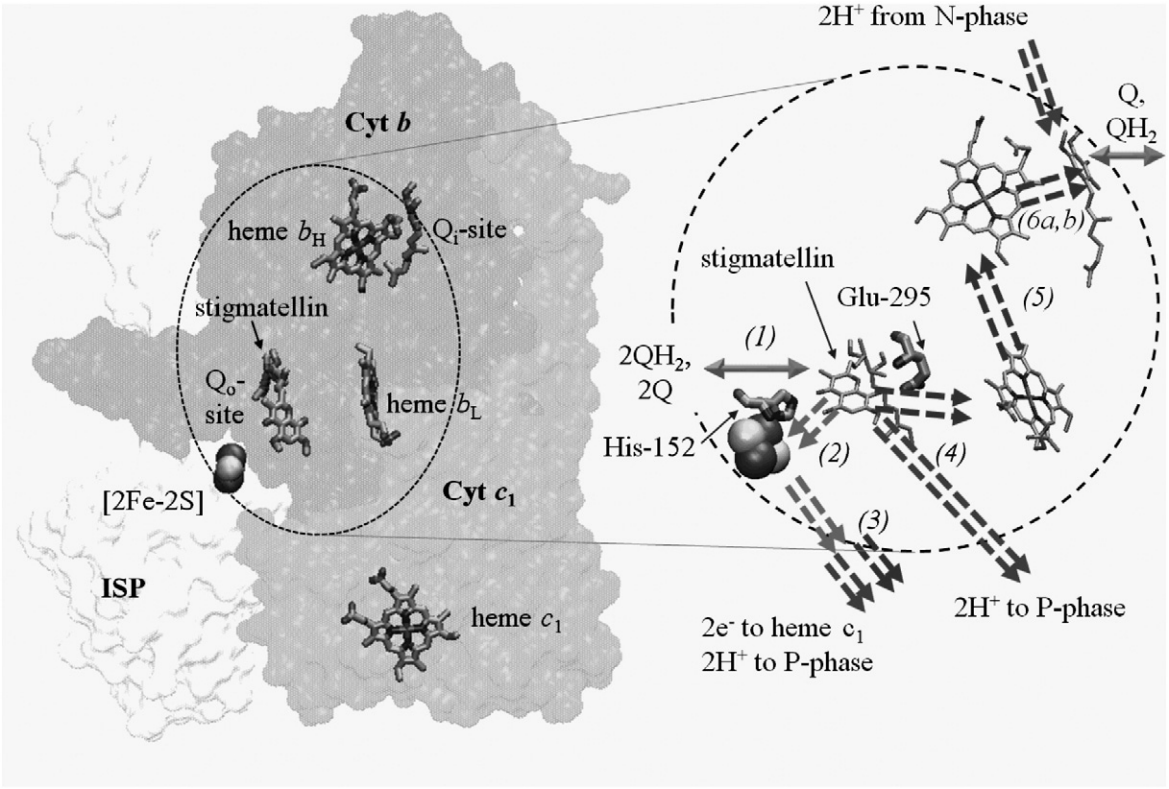

Fig. 1 Monomeric Q-cycle mechanism (adapted from [78]). Left, the subunits of the Rb. sphaeroides bc1 complex monomer, and the prosthetic groups of importance in mechanism (taken from PDB ID: 2QJY). Right, the catalytic core rotated so as to display the main players. The reactions of the Q-cycle are shown by solid arrows (Q, QH2 exchange at catalytic sites), light gray arrows (H-transfers), dark gray arrows (electron transfers) and mid gray arrows (H+ transfers). Stigmatellin bound at the Qo-site shows the position at which the ES1-complex forms. Overall reaction

$$QH_2 + 2\text{cyt } c_2 + 2H_N^+ \rightleftharpoons Q + 2\text{ferrocyt } c_2 + 2H_P^+ + 2H_{chem}^+$$

Chemistry

$$QH_2 + 2\text{cyt } c_2 \rightleftharpoons Q + 2\text{ferrocyt } c_2 + 2H_{chem}^+$$

Transport

$$2H_N^+ \rightleftharpoons 2H_P^+$$

Partial reactions numbered are as follows: *Formation of ES_1*

$$Eb_Hb_L + QH_2 + ISP_{ox} \rightleftharpoons Eb_Hb_L \cdot QH_2 \cdot ISP_{ox} \quad (1)$$

High potential chain. 1st e^- transfer, and formation of ES_2

$$Eb_Hb_L \cdot QH_2 \cdot ISP_{ox} \rightleftharpoons ISPH + Eb_Hb_L \cdot QH\bullet \quad (2)$$

Oxidation of ISPH

$$ISPH + \text{heme } c^+{}_1 \rightleftharpoons ISP_{ox} + \text{ferroheme } c_1 + H_P^+ \quad (3)$$

Low potential chain, starting with ES2. 2nd e^- transfer

$$Eb_Hb_L \cdot QH\bullet \rightleftharpoons Eb_Hb_L^- + Q + H_P^+ \quad (4)$$

Interheme e^- transfer

$$Eb_Hb_L^- \rightleftharpoons Eb_H^-b_L \quad (5)$$

Qi-site reactions

$$Eb_H^-b_L + Q + H_N^+ \rightleftharpoons Eb_Hb_LQ\bullet^-\left(H^+\right) \quad (6a)$$

or

$$Eb_H^-b_LQ\bullet^-\left(H^+\right) + H_N^+ \rightleftharpoons Eb_Hb_L + QH_2 \quad (6b)$$

Note that for complete turnover, the Q_o-site reactions (1–5) have to function twice, and the Q_i-site reactions (6a, 6b) once each. Formation of ES_1 (1) involves second-order reactions with the Q-pool, and binding of the mobile extrinsic domain of ISP_{ox}. These reactions can occur with the complex in a variety of redox states. This term provides a useful descriptor that reflects binding at the Q_o-site without reference to other states of the complex. ES_2 is a useful designator for the initial state from which the second electron transfer proceeds, and is also formed with the rest of the complex in different states. Other partial processes contributing to the formation of ES_1, and complexities in the second electron transfer, are discussed in the text.

ES_2. This allowed ISPH to move away and deliver its electron to heme c_1, and also released QH• in the Q_o-site. The transfer of H^+ from QH• to the carboxylate of E295 would yield the anionic form, $Q^{\bullet -}$, which is the state of dissociation now determined [55]. On the basis of its ENDOR and ESEEM spectra, this is retained in the Q_o-site without spin interaction with N-atoms in the environment. Subsequent rotational displacement of the carboxylic sidechain of E295 would deliver the H^+ to a water chain, allowing its exit to the aqueous P-phase. The sidechain displacement also opened a volume proximal to heme b_L into which the $Q^{\bullet -}$ could migrate by diffusion so as to enhance the rate constant for electron transfer. If $Q^{\bullet -}$ moved to occupy the proximal domain, the electron transfer distance would be some 5 Å shorter than if it occupied the distal domain, leading to a 1000-fold increase in k_{cat} based in a Moser–Dutton distance dependence [47]. The hypothesis was based on several considerations: (i) emerging information from earlier structures from Berry's group showed different configurations (including rotation of the glutamate sidechain) of the Q_o-site when different inhibitors occupied the site [49,50]; (ii) mutations of E295 [54] showed strongly inhibited electron transfer and a weak increase in K_m for QH_2; and (iii) in MD simulations [71], initially to explore mobility of the ISP extrinsic domain, a water chain in the protein was populated on setting up the model, later confirmed in structures [72,73], which contacted the rotated E295 sidechain. Overall, the mechanism allowed the SQ_o intermediate to be kept at a low occupancy, and still to be rapidly removed so as to minimize ROS production while maximizing forward flux [47].

Subsequent studies in other labs have been interpreted as showing that this scenario was hopelessly flawed. Most of the components of the hypothesis have been challenged: the glutamate is not an essential residue, since mutation never leads to a complete block, and in many cases leaves a substantial turnover [74–76]; the pattern of kinetic behavior in E295 mutants indicates that the glutamate is just one component involved in an adaptable mechanism that has a built-in redundancy [74]; the glutamate is not involved in substrate binding [74–77]; the changed pH profile in mutants was interpreted as due to loss of a pK ~6.5 attributed to the glutamate [75,76], implying a role in the first electron transfer; the pattern of pH dependence determined from flash kinetic studies seemed to follow no readily interpretable pattern [74]; kinetic modeling showed that movement of SQ_o in the site was not realistic [56].

In our recent work on additional E295 mutants [10,78], we have addressed these criticisms. The kinetic traces in Fig. 2 show typical data from wildtype and E295 mutant strains through which we have been able to dissect out parameters for partial processes involved in the second electron transfer, and examine their pH dependence. The figure legend includes a summary of protocols used, and further details are given in [78].

3.2.1. The degree of inhibition in E295 mutants

In addressing the degree of inhibition, the critical question is what rate is used as the basis of comparison. In all previous studies, the reference has been the rate of QH_2 oxidation measured in wildtype, either from flash-activated kinetics in bacteria, or from steady-state, or from pre-steady-state measurements with the isolated enzyme using stopped-flow protocols. However, these measurements all reflect the limiting kinetics of the first electron transfer, whereas in our hypothesis, E295 is involved in the second electron transfer. Use of the first electron transfer as the basis of comparison is problematic for another reason; the rate depends on the conditions under which it is determined. In photosynthetic bacteria, the rate measured in situ following flash activation of chromatophore suspensions (~10^3 s^{-1}) is determined in the native membrane environment. When, as in all studies with the mitochondrial enzyme, isolated bc_1 complex is used [75–77], rates measured by stopped-flow mixing are usually at least 10-fold slower, and steady-state turnover is slower still. As a consequence, since the inhibited rates reported in mutants at the -PEWY- glutamate are essentially the same in mitochondrial and bacterial enzymes, the inhibition appears to be much less severe in the isolated complex than when measured in situ. This misleading comparison can lead to mistaken conclusions as to the importance of this residue [78].

Clearly, since the glutamate is involved in the second electron transfer, the intrinsic rate constant controlling that step is the relevant reference. However, the second electron transfer is not normally limiting, and consequently this value is not accessible to direct measurement; it therefore has to be estimated. One approach suggested is to note that the effective rate constant has to compete with the reverse rate constant for the first electron transfer [46–48]; this step is endergonic, but by how much is unknown. Because several partial processes are involved, any more speculative discussion has to be based on specific mechanisms for defined processes, and on occupancies for intermediate states.

In a condensed system, the reactant concentrations that would be appropriate for a second order process have to be replaced by occupancies of states normalized to 1, with first order rate constants defining transitions between states. For example, if the second electron transfer is considered as a simple redox reaction, the reaction can be isolated from other processes through consideration of the change in state involved, $[Q_o^{\bullet -} \cdot b_L] \rightleftharpoons [Q_o \cdot b_L^-]$. Then, the forward electron transfer rate is given by $v = k_2[Q_o^{\bullet -} \cdot b_L]$, where the terms in the square brackets represent occupancies (we ignore complexities in this example, and the backward rate, because the equilibrium constant has to be large enough to pull the overall reaction over). The actual process is certainly more complex, but this simple case serves to illustrate the parameters needed for estimation of the forward rate constant, k_2. These are a measured rate, v, and both SQ_o occupancy and occupancy of oxidized heme b_H, determined under the conditions in which the rate is measured. Although in wildtype the rate is inaccessible (because the first electron transfer is determining), in the more severely crippled E295 mutants, as can be seen from the kinetic traces in Fig. 2, the rates of reduction of the low potential chain are accessible, because they are severely inhibited. In the following sections, we show how these mutants allow us to reach some interesting conclusions: (i) the rate limiting step has clearly changed to reflect some partial process in the second electron transfer; (ii) the mutant strains allow us to estimate parameters determining the rates of partial processes associated with the second electron transfer; and (iii) the parameters can be extrapolated to the wildtype reaction so as to allow development of a detailed kinetic model of the Q_o-site reaction.

3.2.2. Semiquinone occupancy

The endergonic nature of the first electron transfer reaction keeps the SQ_o occupancy low, but until recently, direct experimental evidence for any significant occupancy was lacking. Recent results have provided occupancies under conditions in which SQ_o would accumulate (see below), but the occupancy in normal flux is likely much lower. A maximal value for occupancy under rapid forward flux could be estimated from the lag observed in delivery of the second electron to acceptors. For example, given the limiting rate (v ~10^3 QH_2/bc_1 monomer/s) of the first electron transfer, any lag in reduction of heme b_H attributable to the second electron transfer would be due to the time needed to populate intermediate states at this rate. The states would include the formation of SQ, reduction of heme b_L, and any other intermediate process such as diffusion of SQ. Three groups have studied the kinetics with time resolution good enough to provide useful estimates, all showing a component attributable to the second electron transfer in the range ≥20 μs [4,9,79,80]. In our own work, most of the lag phase (100–120 μs) after photoactivation through the reaction center could be accounted for by the time taken for oxidizing equivalents to find QH_2 at the Q_o-site, in processes occurring before the second electron transfer could start, leaving ≤30 μs unaccounted for, and possibly associated with the second electron transfer. In the Zhu et al.'s work [80], the lag was ~80 μs after mixing, but most of this was likely due to mixing and freezing times. No formation of SQ could be detected in the time during which reduction of ISPH and ferroheme b_L by QH_2 occurred. In the Engstrom et al.'s work [79], oxidation of cyt c_1 was effectively

instantaneous, and the lag in reduction of heme b_H was ~20 μs, but part of this reflected hysteresis in oxidation of ISPH due to its higher E_m compared to heme c_1. Since the shortest lag-phase of 20 μs [79] provides the most critical data, the maximal fractional occupancy of all intermediate states is given approximately by 20/1000 = ~0.02. Since the lag phase also includes other processes, the actual occupancy of SQ states is likely substantially lower. The question of occupancy bears strongly on discussion of kinetic parameters for the second electron transfer (Section 3.2.3).

An antimycin-insensitive signal attributed to SQ_o, which was lost on treatment with British anti-Lewisite (which disrupts the $[Fe_2S_2]$ cluster), had been detected in early studies [81], with occupancy ~0.1 at high pH, but later attempts to detect a SQ sensitive to Q_o-site inhibitors had failed [46,82]. However, four recent reports have re-examined this question, and are of critical interest. Zhu et al. [80] used ultra-rapid-mix freeze-quench protocols, and EPR to assay the changes in reactant concentrations in the first 2 ms of reaction, — a technical *tour-de-force*. Their data were interpreted as showing that no SQ attributable to the bifurcated reaction was formed during the time in which acceptors available in both chains were undergoing reduction. The failure to detect SQ could be explained on the basis of the aerobic conditions of their protocol; Cape et al. [55] were able to assay SQ_o under anaerobic conditions, but detected no SQ under aerobic conditions. However, the time resolution in the Zhu et al. experiment was sub-ms, and it seems likely that they would have seen the SQ if it had been formed at measureable occupancy. Although the authors concluded that no SQ was involved, an alternative interpretation [9] would be that the detection limit was not sufficient to see either SQ, or differences in the ISPH and heme b_L kinetics in the range expected. This is supported by our kinetic model (see [78], and below). If this alternative explanation is correct, their experiment provides a useful constraint, limiting occupancy to the range expected from the lags discussed above, or lower.

Using a rapid-mix freeze-quench approach and the antimycin-inhibited isolated complex from *Rb. capsulatus* under anaerobic conditions, Cape et al. [55] reported occupancy in the range 0.01–0.1 (measured at pH 8). Zhang et al. [57] using flash activation followed by freeze-quench in chromatophores from *Rb. capsulatus*, reported values ≤0.01, measured at pH ~9, where the SQ stability is expected to be maximal. Victoria et al. [78] determined occupancies in wildtype and in one of the glutamate mutants, E295W. Using a rapid-mix freeze-quench approach similar to that of Cape et al. [55], but with the complex from *Rb. sphaeroides*, and a reaction mixture that included excess cyt *c* as acceptor to pull the reaction over, we found values at the high end of their range, with occupancies of 0.03 in wildtype and 0.06 in E295W. We also used flash activation in experiments similar to those in [57], but with *Rb. sphaeroides* chromatophores. However, we found that, if the time of freezing was <50 ms after the flash, at which time the driving force was still close to maximal, the CW-EPR spectra in the $g = 2.005$ range were dominated by the oxidized reaction center, P^+, which had not been visible in the earlier work [57]. As can be seen in Fig. 2, the optic signal for P^+ decayed over the 1–3 s timescale before freezing reported in [57], but this would have substantially decreased the driving force sustaining SQ_o, and this likely accounts for the lower occupancy.

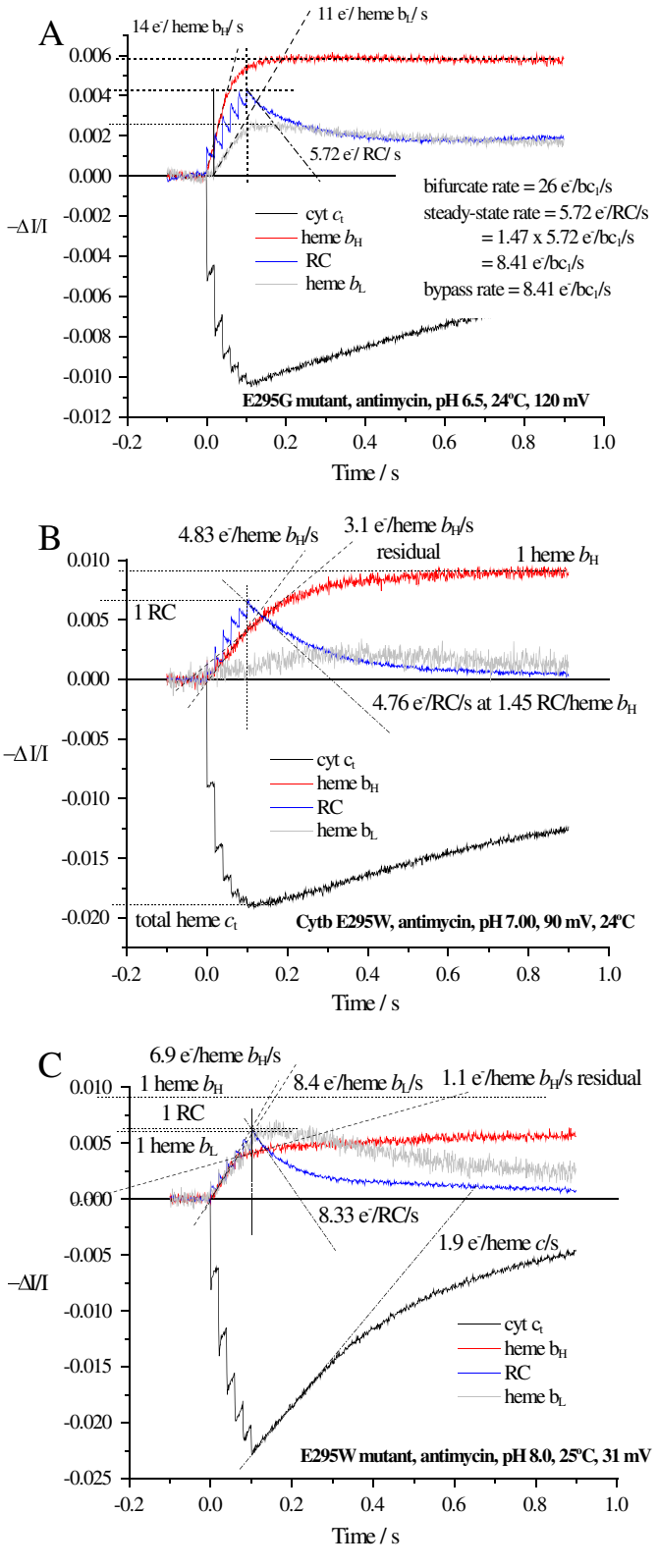

Fig. 2. Kinetics of electron transfer in E295G and E295W mutants. The three frames show kinetics for the components of the photosynthetic chain in cyt *b* mutants at E295 in chromatophores from *Rb. sphaeroides* on illumination by a group of six flashes spaced at 20 ms. For hemes (b_H, red; b_L, gray; $c_1 + c_2$, black) an upward deflection shows reduction. For the photochemical reaction center P^+ (RC, blue), an upward deflection shows oxidation. The rate of the bifurcated reaction is measured through the initial rate of heme b_H reduction. When heme b_H is partly or fully reduced before initiation of turnover by the first flash, the initial rate of heme b_L reduction is added to that for heme b_H. A. E295G kinetics at pH 6.5. E295G shows an intermediate degree of inhibition. At this E_h and pH, the characteristic lag in reduction of heme b_L (no reduction until heme b_H is substantially reduced) can be seen. The poise of the low and high potential chains characteristic of the E_m values is also obvious. B. E295W kinetics at pH 7.0. E295W is the most strongly inhibited strain. The rate of heme b_H reduction is so slow that heme b_L starts to undergo reduction only late in the flash group. The residual bifurcated reaction contributes to the flux detected in re-reduction of the high potential chain. Bypass flux can be estimated by subtraction. C. E295W kinetics at pH 8.0. At this pH and E_h, heme b_H is substantially reduced before the flash, and rates of reduction of both *b*-hemes have to be added to determine the bifurcated flux. Redox changes due to different centers were measures at the following wavelengths: RC, 542 nm; heme b_H, 561–569 nm; heme b_L, 566–575 nm − 0.5 heme b_H (with additional correction for RC and *c*-hemes, depending on stoichiometric ratios); heme c_t ($c_1 + c_2$), 551–542 nm. The apparatus measures, at each wavelength, the normalized transmission change, ΔI/I, which is linear with concentration over small changes.

3.2.3. Rate constant for oxidation of SQ_o

As noted above, in all mutant strains the rate of the bifurcated reaction measured through reduction of heme b_H is markedly inhibited. When the reduction of heme b_L was observed directly (when heme b_H was initially reduced), the rate was similarly slowed (see Fig. 2C). Since equilibration between hemes b_L and b_H is very rapid, the block must be in the step between the formation of SQ_o and the arrival of its electron at heme b_L. This indicates that the limiting step has moved from the first to the second electron transfer, in a step after the formation of SQ_o. This conclusion applies only if the first electron transfer is unaffected by mutation of E295. Earlier work had shown small changes in K_m for QH_2 on the mutation of E295, suggesting weak stabilization of the ES_1-compex [54] which might have affected the QH_2 oxidation rate. In our more recent work, although we could confirm the small effects on K_m previously noted, we found small changes in the opposite direction in other strains. In none of the strains could the small changes have been significant in accounting for the strongly inhibited rates (see Section 3.2.5). On the other hand, the pH dependence of the bifurcated reaction is changed dramatically, and provides important evidence that the controlling step does shift in the mutants (see Section 3.2.4).

In the hypothesis discussed, the movement of SQ in the Q_o-site opens the possibility of electron transfer from SQ_o to heme b_L when the former is located either in the domain of the Q_o-site distal from the heme or that proximal to the heme, with a diffusional step for movement between domains. As noted above, the electron transfer rate is given by $v = k_2[SQ_o \cdot b_L]$, where the terms in the square bracket represent occupancies, but we now have to consider two different rate constants for electron transfer from distal and proximal domains, with rate constants k_{2d} and k_{2p} respectively. We also have to consider the rate constant for the diffusional step, $v = k_{diff}[SQ_o]$, allowing migration of SQ_o between domains, with parameters discussed in Section 4 below.

The severely crippled E295 mutants were slowed enough that the rate, 20–60 $e^- s^{-1}$, could be readily determined over the timescale ($\leq$50 ms) at which SQ_o was measured, and at the same pH of 8.5 [78]. Measurement of these two values in E295W provided the parameters needed for estimation of the rate constant for oxidation of SQ_o by heme b_L, and gave a value for $k_2 < 10^3\ s^{-1}$ [78]. In view of the bulk of the tryptophan substituent, it seems likely that the SQ would have been constrained to the distal domain, so this reflects k_{2d}. A number of mutations to other bulky residues, including E295Q, K, L, showed similar rates for the bifurcated reaction. However, E295W was slower by a factor of 2 suggesting that the bulk of tryptophan might have introduced more pleiotropic effects. The value given for k_{2d} above is based on rates measured in E295Q to take account of this.

Similar kinetic studies provided estimates of rates of bypass reactions, which, over the pH range 6 to 8.0, all showed approximately the same value as the bypass measured for wildtype in the presence of antimycin in this pH range (~5–8 $e^- s^{-1}$). These bypass rates were also similar to the rates of the bifurcated reaction (~10 s^{-1}) measured in the same pH range in the more crippled strains. From this we think that it is likely that, since the SQ_o occupancies are similar, the rate constant from the distal domain must be similar in wildtype to that measured in the mutants.

The empirical value (~$10^3\ s^{-1}$) determined here is 1000-fold lower than the value used in previous discussions of mechanism, calculated from distance using the Moser–Dutton approach. If a value k_{2d} ~$10^3\ s^{-1}$ does apply in wildtype, then, in view of the lower SQ_o occupancy expected under normal forward flux, the value is at least 100-fold too slow to account for the observed rate in wildtype.

Since the rate constant is too low, it is necessary to postulate some process that gets over this limitation. The migration of SQ_o in the site, suggested in our earlier hypothesis [54], provides an attractive possibility, since the rate constant from the proximal domain might be 10^6-fold higher than the k_{2d} ~$10^3\ s^{-1}$ observed. In the hypothesis, the -PEWY- glutamate is involved both in catalysis of proton exit and in facilitation of movement of SQ_o, and mutation could be expected to inhibit either or both processes to explain the slowed rate.

3.2.4. Dependence on pH

The rate of QH_2 oxidation from mitochondrial or bacterial bc_1 complexes follows a bell-shaped pH profile, first analyzed by Brandt and Okun [63] as a curve well fit by two pK values in the range pK_{app} ~6.6 (for the rising side) and pK_b ~9.2 (for the falling side). Redox titration of ISP [83] had revealed a complex pattern as a function of pH, interpreted as showing two pK values for the oxidized form, pK_{ox1} ~7.6 and pK_{ox2} ~9.6, and two pK_{red} values >10. Brandt and Okun [63] concluded from the disparity between values that pK_{ox1} did not contribute to the kinetic behavior. When the structures became available showing His-161 (in mitochondria, equivalent to His-152 in *Rb. sphaeroides*) as a ligand to stigmatellin, and likely also to QH_2 in ES_1, it became obvious that the pK_{app} ~6.5 might be associated with pK_{ox1}, but displaced by the binding energy [51]. This was strongly supported in our later work with mutant strains in which both E_m and pK values were changed. In a set of such ISP mutants, we could interpret the behavior in terms of Eq. (7). All measured rates could be fit using fixed values for all parameters except for the variables pK_{ox1} and ΔG^o_{ET}, given by the pK and E_m values experimentally determined [13]. As already noted, since changes in pK_{app} always tracked changes in pK_{ox1}, it seems well established that the pK_{app} ~6.5 is associated with the involvement of the dissociated form of His-152 in the formation of ES_1.

In this light, it is interesting to review the outcome of experiments with strains mutated at the -PEWY- glutamate. As noted above, in such mutants, the pH profile of the Q_o-site reaction was modified [74,76,77]. In the more weakly inhibited strains, pK_{app} was shifted to higher pH values, and in the more crippled mutants, the pK_{app} ~6.5 was largely lost. In other labs, this was interpreted as showing that pK_{app} ~6.5 was a property of the glutamate lost in the mutants [76,77]. In our own recent work [78], we found a similar pattern, but pointed out that attribution of the pK_{app} ~6.5 to the glutamate was contrary to our assignment to pK_{ox1} of ISP. We suggested instead that the loss of this pK reflected a change in the rate limiting step from the first to the second electron transfer, which would minimize dependence on the parameters of Eq. (7). In our hands, the new pH profile was dominated by a pK ~8.5 leading to an increase in rate. We attributed this to a participant in the second electron transfer, tentatively the dissociation of $QH^\bullet \rightleftharpoons Q^{\bullet -} + H^+$, with the anionic form as the electron donor to heme b_L. The pH dependence of SQ_o has not yet been determined directly in any system, but in [55], the anionic form was fully present at pH 8.0, suggesting a pK much lower than 8.5 in wildtype. Perhaps the high value seen in the mutant strains might reflect an *indirect* change due to loss of the carboxylate [78].

The question of dissociation status of SQ_o opens up a wider discussion of just where the second step is blocked. Mutation of E295 might be expected to inhibit either or both of the processes catalyzed, — proton exit and the enhancement of rate constant by migration. Any change that hindered the migration of SQ in the site would frustrate diffusion to the proximal domain. If our interpretation of the pK ~8.5 is correct, then the SQ is already in the anionic form when the low rate is determined in E295W, so the proton has already gone, and the block must be in the electron transfer step. However, this should not be taken to indicate that the proton exit is uninhibited. It seems quite possible that both steps are inhibited to similar extents, and that either one or the other could be the controlling step in different mutants. The topic is discussed in some detail in [78].

3.2.5. Effect of mutation at E295 on QH_2 binding

In our earlier work [49,54], we had found a weak effect on QH_2 binding in two mutants, E295D and E295G, in which the apparent K_m was increased by ~2-fold, and suggested that this might indicate a weak ligand between E295 and the QH_2 substrate, compatible with the nature of ES_1 suggested by inhibitor binding [54]. Such a role would be

expected to lead to a direct effect of mutation in the first electron transfer. Subsequent work in other labs [74–77] has shown little or no effect of such mutations on K_m measured more directly. In our more recent work, we found the same weak effects in other mutants but of variable sign [78]. From this we concluded that there was no evidence for any substantial involvement of E295 in the binding of substrate, and that the small changes in affinity could not in any way account for the dramatic changes in rate. Note that this lack of effect on binding of QH_2 in no way precludes a role either in H-bonding to QH•, the substrate for the second step, or as acceptor for H^+ in catalysis of QH• dissociation.

3.3. Parameters related to SQ_o occupancy

In addition to a rate constant for transfer from the distal domain, knowledge of the occupancy allows calculation of a number of important parameters for the Q_o-site reaction. The overall driving force for the Q_o-site reaction is given by:

$$\Delta G'_{overall} = -F\left\{\left(E'_{highPC} + E'_{lowPC}\right) - 2E'_{Q/QH_2}\right\}. \quad (10)$$

Since the flux in the antimycin-inhibited wildtype system is minimal, the high potential chain (highPC) and the low potential chain (lowPC) will come close to equilibrium, both separately within a chain, and together with the driving force. The quasi-equilibrium after a group of six flashes to excite chromatophores is described in terms of visible components by Eq. (10), and by $E'_{ISP} = E'_{cyt\ c_1} = E'_{P+} = E'_{highPC}$, and $E'_{heme\ b_L} = E'_{heme\ b_H} = E'_{lowPC}$. Then the E' values for the two SQ couples can then be determined from $E'_{SQ/QH2} \sim E'_{highPC}$ and $E'_{Q/SQ} \sim E'_{lowPC}$, and their difference would contribute to the overall free-energy through Eq. (10). Values for these terms can be taken directly from the experimental E_h, and from kinetic traces like those in Fig. 2, to give $E'_{Q/QH2} \sim 90$ mV (for the Q-pool), $E'_{P+} \sim E'_{SQ/QH2} \sim 500$ mV, and $E'_{heme\ b_L} \sim E'_{Q/SQ} \sim -320$ mV. Since $[QH_2]$ can also be estimated, we can get $E_{m\ SQ/QH2} \sim 570$ mV by using $E' = E_m + 59 \log_{10} \frac{[SQ]}{[QH_2]}$ (with [SQ] ~0.06), and an equilibrium constant for the first electron transfer, $K_1 \sim 10^{-4.5} \sim 0.00003$. With the Q-pool as reference, $E_{m\ Q/SQ}$ is then ~ −390 mV, the equilibrium constant for the second electron transfer is $K_2 \sim 10^5$, and the overall equilibrium constant, $K_{overall} \sim 3.5$ — the value obtained directly by substitution of E_m values in $\Delta G'^{o}_{overall} = -F\left\{\left(E'^{o}_{ISP} + E'_{heme\ b_L}\right) - 2E'^{o}_{Q/QH_2}\right\}$. These values provide a framework for detailed kinetic simulation as discussed in Section 4.

Our determination of SQ_o occupancy also allows calculation of rate constants for bypass reactions in the antimycin-inhibited complex. The main reactions of interest are: (i) electron transfer from SQ_o to O_2 or the high potential chain, with v_{HP}; and (ii) the reduction of SQ_o by heme b_L^-, with v_{LP}. This latter contributes to reaction (*c*) in the following sequence:

$$QH_2 + ISP_{ox} \cdot b_L \cdot b_H^- \rightleftharpoons Q \cdot ISPH \cdot b_L^- \left(H^+\right) \cdot b_H^- \rightleftharpoons Q + ISPH \cdot b_L^- \left(H^+\right) \cdot b_H^- * \rightleftharpoons ISP_{ox} \cdot b_L^- \cdot b_H^- + cyt\ c^- + 2H^+ \quad (a)$$

$$QH_2 + ISP_{ox} \cdot b_L^- \left(H^+\right) \cdot b_H^- \rightleftharpoons SQ_o \cdot ISPH \cdot b_L^- \left(H^+\right) \cdot b_H^- * \rightleftharpoons SQ_o \cdot ISP_{ox} \cdot b_L^- \left(H^+\right) \cdot b_H^- + cyt\ c^- + H^+ \quad (b)$$

$$SQ_o \cdot ISP_{ox} \cdot b_L^- \left(H^+\right) \cdot b_H^- \rightleftharpoons QH_2 \cdot ISP_{ox} \cdot b_L \cdot b_H^- \rightleftharpoons Q + ISPH \cdot b_L^- \left(H^+\right) \cdot b_H^- * \rightleftharpoons ISP_{ox} \cdot b_L^- \left(H^+\right) \cdot b_H^- + cyt\ c^- + H^+. \quad (c)$$

(The * indicates cyt c_{ox} entering the reaction. (H^+) is assumed to equilibrate with the P-phase). Reaction (*a*) starts with b_L oxidized, and primes the system through the normal Q-cycle; reactions (*b*) and (*c*) represent the bypass, which repeats in the antimycin inhibited steady-state. Overall, reaction (*b*) plus (*c*) gives $QH_2 + 2cyt\ c_{ox} \rightleftharpoons Q + 2cyt\ c^- + 2H^+$, the "chemical" component left when transport processes are subtracted from the overall reaction (see Fig. 1 legend). Reduction of SQ_o through (ii) (the reaction on the LHS of (*c*)) was suggested by Muller et al. [40], and could itself lead to bypass if SQ left the site to disproportionate. Osyczka et al. [43] discussed the alternative fate through the normal forward reaction. Note that reduction of Q_o by heme b_L^- is a reversal of the second electron transfer, necessarily included in a reversible Q-cycle, and contributing to bypass reactions only in so far as SQ_o participates. In principle, any state with SQ_o could pass electrons directly to O_2, or the high potential chain through (i).

Since in the more crippled mutants, combined rates for these bypass reactions are similar to those for the bifurcated reaction [78], they could be derived from the parameters determined above through $v_{HP} = k_{HP}[SQ_o] \cdot$[2nd reactant] ~5 s^{-1}, and $v_{LP} = k_{LP}[SQ_o \cdot b_L^-]$ ~5 s^{-1}. Under aerobic conditions, SO formation saturates at ~10^{-4} M O_2 [40], and with heme b_L fully reduced the value for k_{HP} would be in the range $10^7 M^{-1}\ s^{-1}$. In the absence of O_2, the local activity of the second reactant (the appropriate configuration of ISP_{ox}), is unknown, so speculation must be limited. The value for $k_{LP}[SQ_o]$ would have to be ~$10^2\ s^{-1}$. It is likely that these empirical rate constants pertain to processes that are gated, but details of mechanism remain to be determined.

4. A kinetic model for the antimycin-inhibited complex

We have used kinetic simulation to demonstrate that the reaction mechanism suggested is plausible. The model is described in detail in [78], which also includes scripts for implementation in the Dynafit software package [84]. In contrast to recent models implemented using the Gillespie algorithm [85–87], we have separated several processes treated there as single reactions into partial processes. In the formation of ES_1 we have taken account of the ~10-fold displacement in favor of QH_2 binding indicated by $\Delta E_m^{(ES\text{-}free)}$ (see Eq. (8)) [78]), and we adjusted the p*K* in the Brønsted relationship to reflect pK_{app}, appropriate for involvement of the bound ISP_{ox}. In the first electron transfer, we have included the partial processes implicit in the Marcus–Brønsted treatment outlined above. In the second electron transfer, we have included a diffusional step for the migration of SQ_o from distal to proximal domains of the Q_o-site, and have assigned a rate constant $k_{diff} > 10^7\ s^{-1}$, based on a 6 Å 1-D path, and a diffusion coefficient in the range 10^{-7} to $10^{-9} cm^2\ s^{-1}$, taken from the literature [88,89]. For the electron transfer rate constants from distal and proximal domains, respectively, we used $k_{2d} \sim 10^3\ s^{-1}$, the empirical value obtained from SQ occupancy, and $k_{2p} \sim 10^9\ s^{-1}$, obtained using a Moser–Dutton treatment of distance dependence (but respecting the caveats below). All equilibrium constants in the model are well-justified, and define appropriate ratios for forward and reverse reactions. However, for one process, we found it necessary to introduce artificially high rate constants to generate overall reaction rates observed. This is the reaction by which electrons are removed from the high potential chain. We believe that this artificial device might indicate that some cryptic gating process introduces control in the high potential chain. Similarly, although parameters determining bypass processes could be introduced along the lines outlined in Section 3.3 above, they would not represent defined partial processes, and we have therefore omitted such terms.

The model simulates kinetics that match those measured in both bacterial and mitochondrial complexes, and reproduces the thermodynamic constraints expected from the modified Q-cycle [2,25] (Fig. 3).

From the simulation we also obtain information about occupancies of intermediate states that are not readily measured, including SQ_o occupancy in the normal forward flux (Fig. 3C, D). In order to match maximal forward rates (with heme b_L fully oxidized), the effective rate constant for oxidation of SQ_o must be in the range $k_2 \geq 10^7\ s^{-1}$; in the simulation, k_{diff} becomes the limiting step as it is lowered below this.

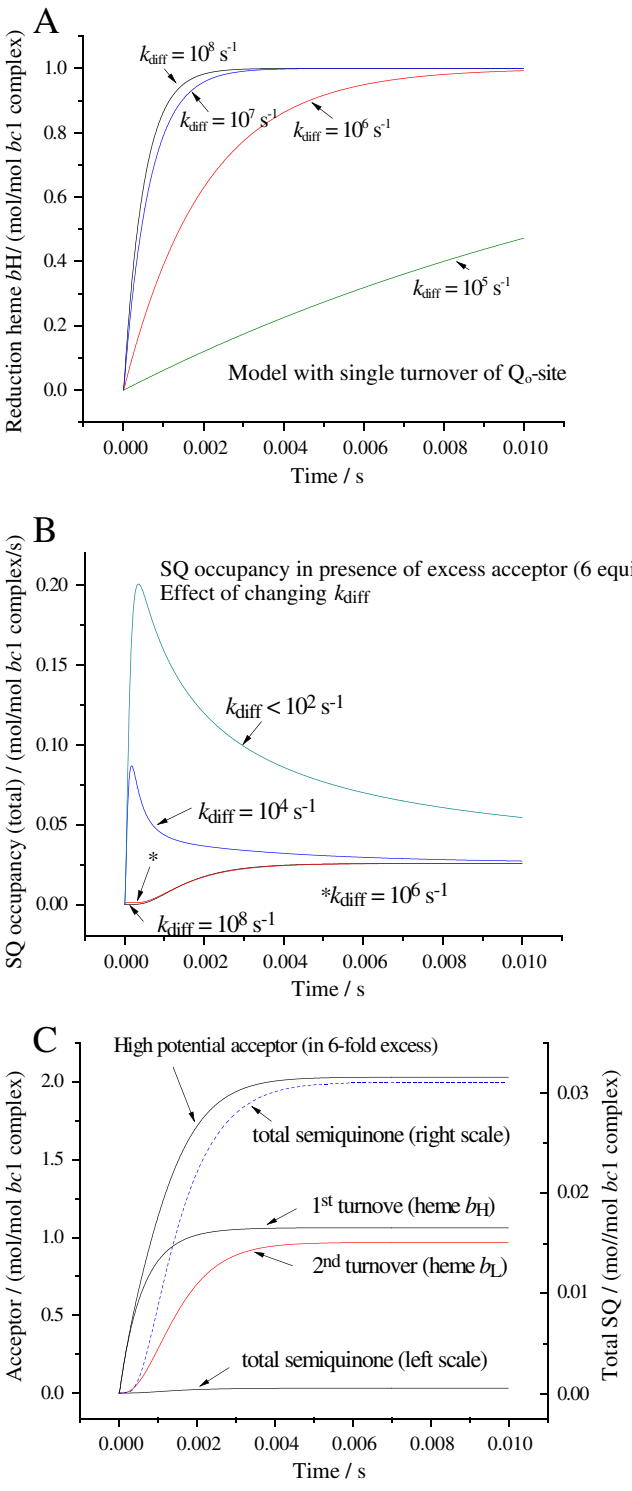

Fig. 3. Simulated kinetics showing features characteristic of electron transfer in the antimycin-inhibited complex. Details of parameters and scripts for implementation in Dynafit [81] are given in [81]. A. Reduction of heme b_H during the first turnover in the absence of added acceptor. The effects of mutation of E295 are simulated by slowing the diffusion of SQ_o between distal and proximal domains of the Q_o-site through lowering the rate constant. Although the path may be crooked, the diffusion was assumed to be essentially a 1-D process, with a distance of 6 Å, and a diffusion coefficient taken from the literature (see text for references). B. Occupancy of SQ_o when excess of acceptor was present to allow multiple turnovers. The effect of mutation of E295 is simulated by lowering the rate constant for SQ diffusion as in A. C. The overall reaction is 'measured' through the kinetics of reduction of the acceptor from the high potential chain (physiologically, cyt c_2), and of the *b*-hemes. Significant occupancy of SQ_o occurred as the third QH_2 was oxidized in a partial turnover. Conditions as for B, but note the different scale. The dotted trace shows SQ_o at a more sensitive scale (right ordinate).

With $k_{diff} > 10^7\ s^{-1}$, the SQ_o occupancy is $<10^{-4}$, below current resolution limits; from Fig. 3B, with $k_{diff} = 10^8\ s^{-1}$, the occupancy is $<1.6\times10^{-5}$, and if the frictional coefficient in the site was lower than in the membrane, an even lower value could be justified. In the antimycin-inhibited wildtype complex, the occupancy only becomes appreciable as heme b_L becomes reduced (Fig. 3C), and reaches the value seen experimentally only as the site turns over for a third time (starting with the oxidized complex). Significant inhibition is seen only as the limiting rate constant is reduced below $10^6\ s^{-1}$, so whenever the second step becomes rate determining ($\nu < 10^3\ s^{-1}$), this likely already represents a substantial inhibition. As k_{diff} is lowered, SQ_o occupancy becomes transiently higher than so far detected (as high as 0.2 in Fig. 3B), but eventually falls to the same level as seen in the wildtype (~0.03). This is because the transiently high occupancy falls as the residual low rate of SQ_o oxidation from the distal domain (determined by k_{2d}) allows the Q_o-site reaction to come to the same equilibrium with high and low potential chains as in the wildtype.

4.1. Some considerations in the application of Marcus-type treatments

The rate constants used in the kinetic model are either empirical, or derived from theory using well-established principles. In applying Marcus-type treatments, we have used the Moser and Dutton distance dependence [90–92], but with attention to the following caveats.

(i) We have avoided the use of the Hopfield approximation [93], which leads to the factor 3.1 in the standard Moser–Dutton equation [92]. The Hopfield approximation was introduced as a quasi-quantum mechanical term to account for the behavior at low temperatures, in which the dependence of electron transfer rate departs from the Arrhenius slope, and becomes independent of T [94]. The Boltzmann term k_BT is replaced by the term $\hbar\omega/2\ \coth[\hbar\omega/2k_BT]$, which has the value 3.1 when $\hbar\omega = 0.056$ eV, and $k_BT = 0.025$ eV (at 290 K). This expression has the property that it approaches k_BT at high temperature ($k_BT \gg \hbar\omega/2$), while at low temperature it approaches $\hbar\omega/2$, which is independent of temperature [94]. It was adopted in the Moser–Dutton treatment because it gave a good empirical fit to early data through which the approach was developed [95]. Unfortunately, this treatment is incompatible with detailed balance [9,96], and should therefore be avoided. We use instead the classical 4.23 ($= F/(4\times2.303RT)$) to scale the Marcus term.

(ii) For similar reasons, we also avoided the Page approximation [97], which, in the endergonic range, aims to correct curves generated by use of the Hopfield approximation, but which lacks algebraic consistency [9,96].

(iii) We have used the simple distance dependence only for partial processes that are simple electron transfers. In the Marcus–Brønsted treatment for the first electron transfer, the distance through the bridging histidine is ~7 Å, giving $k_{ET1} \sim 10^8\ s^{-1}$, but this is convoluted with the equilibrium constant given by the Brønsted term for distribution of the proton, $K_{proton} \sim 10^{-5}$, to give the observed rate constant $\sim 10^3\ s^{-1}$. In the second electron transfer, the rate constant given by distance (~11.5 Å) for oxidation of SQ_o from the distal domain by heme b_L would be $k_{2d} \sim 10^6\ s^{-1}$, and the 1000-fold difference from the empirical value ($k_{2d} \sim 10^3\ s^{-1}$) discussed above likely reflects convolution with processes associated with proton exit and SQ movement, in which the -PEWY- glutamate is involved. However, the reaction from the proximal domain is likely a simple electron transfer, with $k_{2p} \sim 10^9\ s^{-1}$ for a distance of 6.5 Å, — the value used in the simulation.

4.2. Temperature dependence

A penalty for avoiding the Hopfield approximation is that the neat explanation for the loss of temperature dependence at low T also has

to be abandoned. It seems worthwhile to consider alternative approaches. As is well known, in Marcus' early treatment [98], he separated the reorganization energy, λ, into two parts, λ_i and λ_o for inner-shell atoms and the contributions from outer molecules in the surrounding solvent, respectively. The inner-shell term, λ_i, is that leading to the Hooke's law treatment and the parabolas for displacement from equilibrium of vibrational coordinates through which the single-valued reorganization energy is generally represented in simple treatments [94]. While use of a single-valued λ clearly gives a useful simplification, it ignores Marcus' outer-shell term. Marcus derived λ_o from the following Born-type expression:

$$\lambda_o = \frac{\Delta e^2}{4\pi\varepsilon_o}\left(\frac{1}{2r_1}+\frac{1}{2r_2}+\frac{1}{r_{12}}\right)\left(\frac{1}{D_{op}}-\frac{1}{D_s}\right)$$

in which r_1 and r_2 are radii of reactants when in contact, r_{12} is $r_1 + r_2$, and the D_{op} and D_s terms on the right are dielectric constants, — respectively, the optical dielectric contribution (the square of the refractive index) and a static term for the surroundings (the 'medium' in Marcus' treatment). In the present context, it is useful to recognize that D_s is a property of a particular environment, and has a particular value (so that λ has a particular value) only at a particular temperature. The value is static only at T = 0. It is never a single-valued function, because the dielectric response is not only dependent on the nature of the medium, but also both on the timescale of the reaction and on temperature [99,100]. The value of λ_o is singular only at temperatures where non-optical components of dielectric response have been frozen out — the range over which electron transfer becomes independent of temperature. Similarly, the components of D_s have time constants dependent on the process involved in the dielectric response. For very fast electron transfers, the D_{op} component would be important, since components requiring significant nuclear displacements would be too slow to respond. Note that although, from the Franck–Condon principle, the electron transfer process itself is essentially instantaneous in this context, the reorganization energy reflects the probability for the system to find itself in the configuration appropriate for this event. The dielectric response is therefore determined by the time over which a particular process can occur, and the dielectric components that can respond in that timescale. These dependences of dielectric response on timescale and temperature mean that D_s (and therefore λ) has a particular value for a particular electron transfer only under defined conditions. It is a dynamic function in any process (for example, following photoactivation of reaction centers) involving sequential electron transfers on different timescales. Similar considerations might also apply to the complexes of respiratory or photosynthetic chains; the local environmental contribution to λ depends on the time constant of the electron transfer process, and on the temperature at which it is measured. These factors have been recognized in the reaction center community, where they are more accessible to experimental test (cf. [101–103]), but are perhaps less appreciated elsewhere. Krishtalik [104] has also recently discussed this topic, and it will be interesting to see how such treatments can be extended to a more formal representation of dependence of λ on timescale and temperature over a wider range.

With the above caveats, the kinetic model successfully simulates the behavior and properties of the antimycin-inhibited bc_1 complex, as

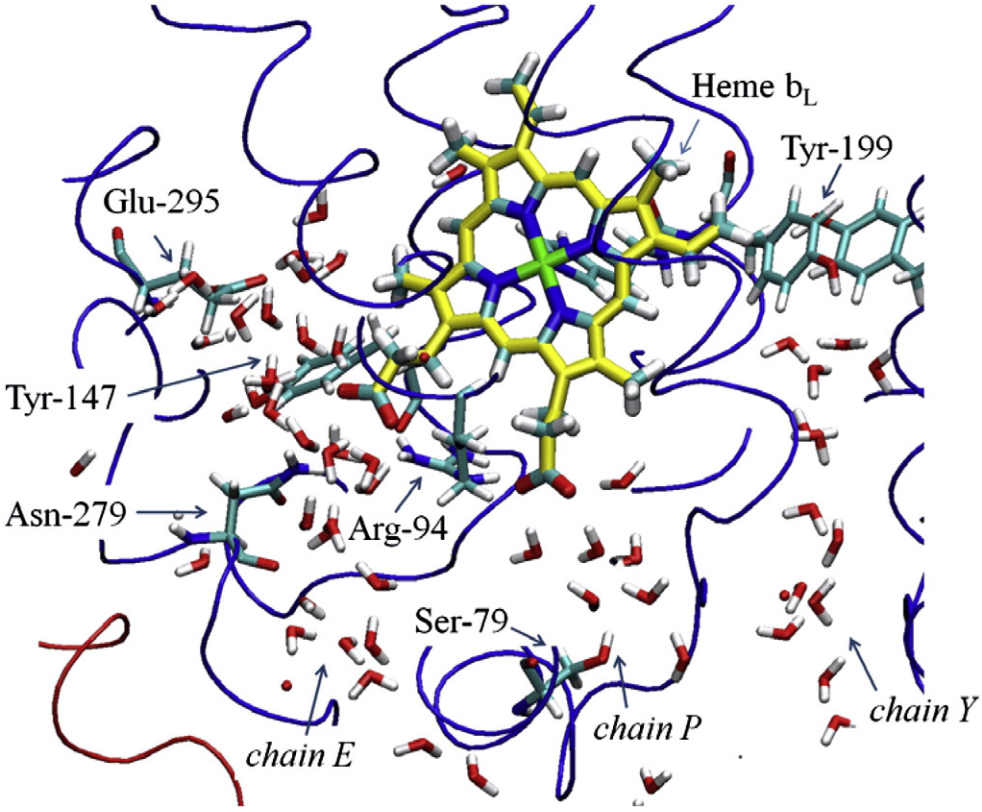

Fig. 4. Water chains, modeled in the *Rb. sphaeroides* bc_1 complex, that connect the environment of the Q_o-site and heme b_L to the P-side aqueous phase. The structure of the protein sliced in the plane of heme b_L was selected to show features of interest, including waters within 12 Å of the heme. The water chains might be involved in equilibration of reactants, protein, and prosthetic groups with the H^+ activity of the aqueous phase (at bottom). *ChainE* connects E295 and the Q_o-site, to Arg-49, a ligand with one of the heme propionates, and to the P-phase; *chainP* connects to the other heme propionate; *chainY* connects to the Tyr-199 pair at the dimer interface, but its mechanistic role is unknown. Also shown are the locations of residues discussed in the text, including those thought to stabilize *chains E* and *P*. In this simulation, the Q_o-site was vacant. See text for further explanation. (This image was made using the VMD software, from an MD simulation run under NAMD, both packages developed with NIH support by the Theoretical and Computational Biophysics group at the Beckman Institute, University of Illinois at Urbana-Champaign.)

exemplified in Fig. 3. However, the simulation avoids complexities associated with gating. Such processes must also operate within natural constraints.

5. Control and gating of the Q_o-site

Osyczka at al. [43] pointed out that the Q-cycle would be decoupled unless some mechanism prevented short circuit reactions from occurring. Although they favored a concerted mechanism, the involvement of SQ seemed well established from our own work [40], and, as already noted, SQ species with the expected properties have since been demonstrated [55,57,78]. We will therefore restrict consideration to gating mechanisms. In the kinetic model (Section 4) the complexities of the second electron transfer are simplified by representing mutation of E295 through a modulation of the value for k_{diff} in the diffusion of SQ_o from distal to proximal domains. This seems to simulate the observed behavior, but at the expense of any representation of partial processes involved in the catalysis of proton exit. Since these processes are likely at the heart of gating and control, the model could obviously be improved. For the current model, such simplification is necessary because we know little about the partial processes involved.

5.1. Water chains for proton exit

Gating through reorientation of water dipoles in response to changes in heme charge has been suggested in cytochrome oxidase [105] and in the bc_1 complex [43]. The intermediate states in proton exit are not populated under equilibrium titration, and transition rates must be rapid compared to the limiting step under normal forward chemistry. They are therefore not readily measured kinetically, and parameters are inaccessible. In order to address this problem, we have started preliminary work to investigate putative proton exit channels. We have set up the *Rb. sphaeroides* bc_1 complex structure for molecular dynamics (MD) studies in a model membrane with aqueous phases. Population of the protein model with waters revealed several potential water chains associated with Q_o-site and heme b_L, including *chainE*, previously identified as a proton exit pathway [54] (Fig. 4). Examination of the structures showed that the water chains were stabilized by H-bonding interactions with protein, including sidechains and backbone –NH and ═O atoms. Most of these buried waters are not resolved in the structures, but in MD simulations in the NAMD environment, the chains shown in Fig. 4 are stable, although individual waters exchange rapidly. The MD simulations enable us to identify residues in *chainE* suitable for mutation to test their role in stabilization of the chain. Some of these sites, Glu-295 [54,74,76,77] and Tyr-147 [106], have been subject to previous mutational analysis, but we are exploring these and others, including Asn-279, Arg-94, and Ser-79 in the current work, to identify a kinetic profile consistent with a functional role in proton exit.

The traces of Fig. 5 show results from Asn-279 mutants from which such a role seems likely. We compare the rates of Q_o-site turnover on the first (monitored through reduction of heme b_H) and on the second flash (monitored through reduction of heme b_L), in wild type and a number of different mutants (N279D, I, F shown). The rates after flash1 and flash 2 were similar in wildtype. In the mutants, the rate after the first flash was about 50% inhibited with respect to wildtype, but the rate was more strongly inhibited after the second flash. The inhibitory

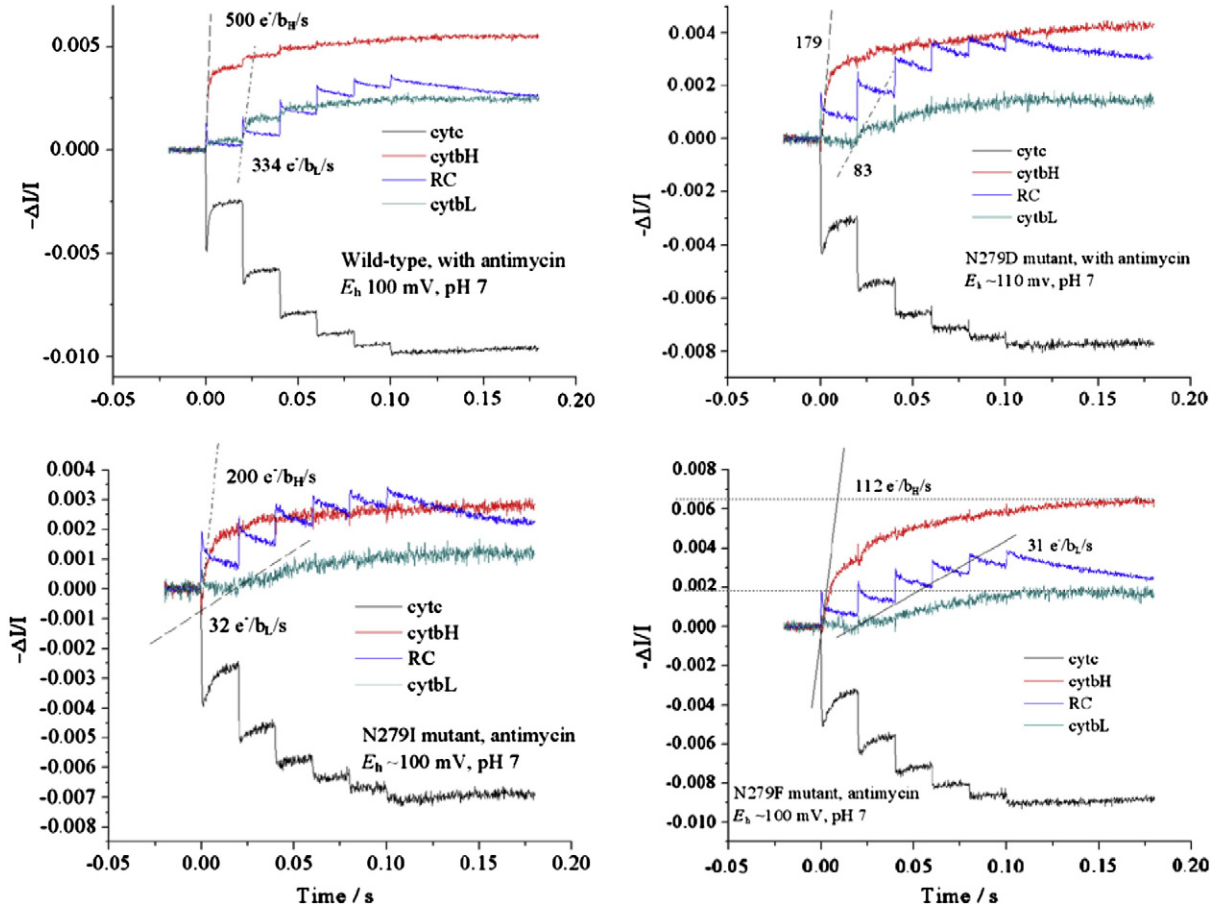

Fig. 5. Kinetics of the bifurcated reaction in N279 mutants. Behavior interpreted as inhibition by blockage in the water *chainE* for proton exit, as seen in the presence of antimycin on excitation by a group of 6 flashes. Oxidation of the first QH_2 is assayed by the rate of heme b_H reduction on the first flash (red trace); that of the second QH_2 by the reduction of heme b_L on the second flash (dark green trace); traces for RC (blue) and cyt c_1 plus c_2 (black) show kinetics in the high potential chain. Chromatophores from *Rb. sphaeroides* were incubated in an anaerobic cuvette poised at 110 mV, pH 7.0, in a medium with 100 mM KCl, 50 mM MOPS buffer, with a cocktail of redox mediators [112].

affect after the second flash was greater in mutants with an apolar residue. In the present context, this might be explained if E295 was available to accept the proton released on the first turnover, but could then not deliver it to the aqueous phase, because of a block at the mutated N279. In that case, the E295 carboxylate state and the acceptor function would not be restored, so that the QH• from the second turnover would have nowhere to donate its proton. When these mutations were generated in silico, the MD simulation showed that *chainE* was no longer continuous or stable, with the break at the mutation site. From these results we feel confident that this pathway is essential for rapid proton exit.

5.2. Gating in the first electron transfer

Coulombic effects are likely much more significant for reactions within the protein matrix, for which the local dielectric constant will be low (D in the range 4 to 15), than for those in direct equilibrium with the aqueous phase (D ~80). Since in the first electron transfer, the reduction of ISP_{ox} leads to transfer of an electron and a proton, and is therefore neutral, the proton and electron likely part company on oxidation of ISPH by heme c_1, effectively in water, with no electrogenic, and little coulombic consequence. It seems unlikely that significant control could be exerted by changes in coulombic interactions in the first step of electron transfer. However, although movement itself is likely too rapid to mediate control, interactions of ISP at the two interaction sites, and conformational changes, have been much discussed as control functions.

The most obvious conformational changes are the movement of ISP to deliver the electron to heme c_1 [6,54] and the rotation of E295 already discussed above. Careful studies of the structures have revealed other interesting changes on binding of different inhibitors, both in the Q_o-site and in docking interfaces. These offer rich opportunities for speculation as to control in the first electron transfer [51,107,108], and have recently been nicely reviewed by Berry and Huang [109]. Perhaps most interesting, and among the first to attract attention [49–51,53,54], was the change seen between structures with stigmatellin in the distal domain forming a complex with ISPH, and those with myxothiazol or other MOA-type inhibitors in the proximal domain. With the proximal domain occupants, the volume of the Q_o-site closer to the heme expanded, while the opening to the site (through which interactions with ISPH occur with distal domain occupants), became closed by displacements in the -PEWY- loop (the "-PEWY- see-saw" [51]) and several of the helices lining the site [72,107,109]. As a consequence, a "trapdoor tyrosine" (Tyr-302 in *Rb. sphaeroides*, Tyr-279 in chicken) moved to close the access port. In structures with distal domain occupants, the interaction with ISPH pulls the trapdoor open, and Tyr-302 forms an H-bond to ISP Cys-151 backbone carbonyl, stabilizing ISPH in the *b*-position [71]. Mutations at this tyrosine in *Rb. sphaeroides* led to inhibition of electron transfer, markedly in Y302G and Y302Q [51]. Spontaneous or inherited mutations at this site in mitochondrial complexes cause severe exercise intolerance and "multi system disorders" in humans [110], and tolerance in *Plasmodium falciparum* to atovaquone in the treatment of malaria [111]. Lee at al. [108] have recently studied additional mutations at Y302 in *Rb. capsulatus*, and demonstrated increased ROS production, and formation of a disulfide cross-link with ISP C155 in the Y302C mutant, with more dramatic inhibitory effects.

It seems likely that reconfiguration of the docking domain would disfavor binding of ISP at the Q_o-site interface under circumstances in

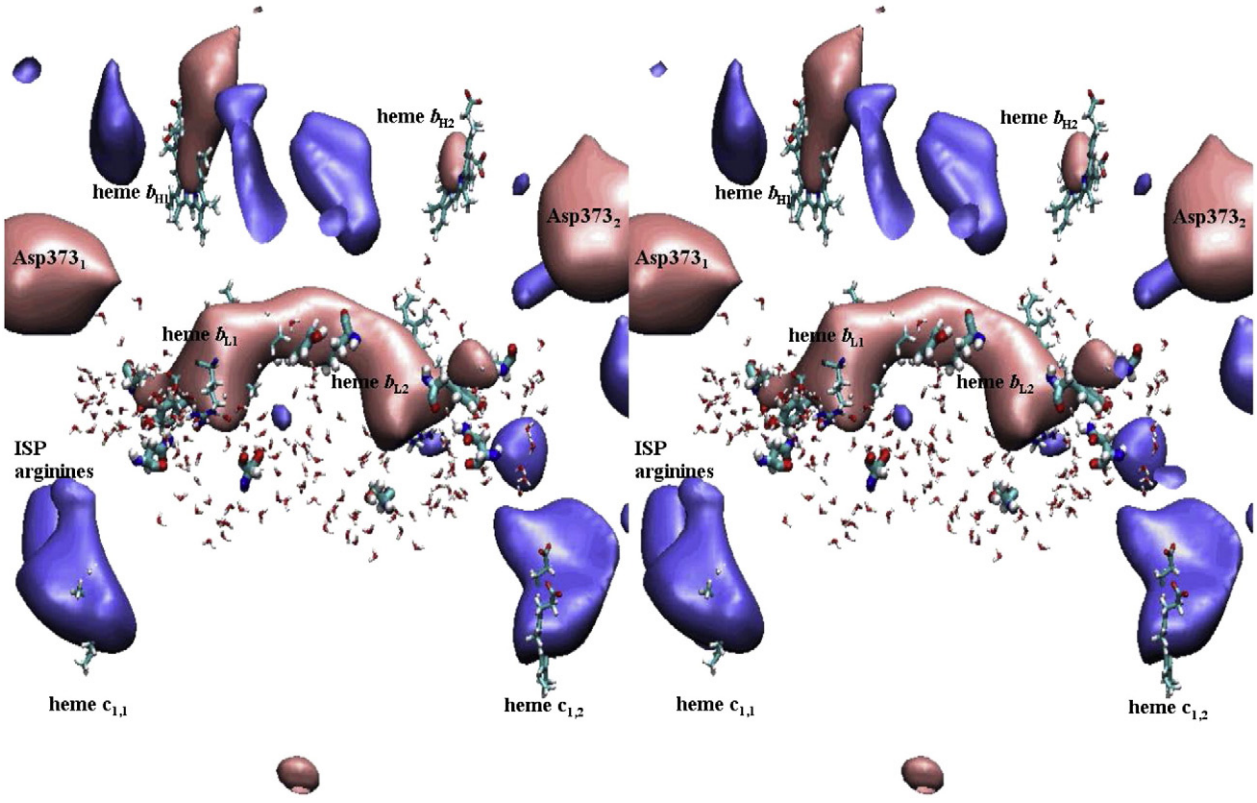

Fig. 6. Electrostatic profiles for the reduced bc_1 complex dimer. Selected isopotential contours for positive (blue) and negative (red) potential are displayed. Because the hemes are all reduced, differences in the isopotentials are determined by the protein environment. The central red dumbbell encompasses the reduced b_L hemes, and bridges the dimer interface, with the more negative protein potential perhaps accounting in part for the failure of electron transfer between the hemes. The weaker negative surfaces of smaller volume above are the b_H hemes; the pathway between hemes b_H and b_L is close to neutral in potential. The more pronounced peripheral blobs are due to Asp-373. The positive potentials (left and right at bottom) are the c_1 hemes, and arginines in one of the ISP subunits (the other is off scale). The water chains detailed in Fig. 4 and critical residues in the vicinity of heme b_L are shown. (Stereo pair for crossed-eye viewing; electrostatic profiles were calculated using PME electrostatics analysis in VMD, and are displayed as two isosurface representations. (This image was made using the VMD and the NAMD software, see Fig. 4 legend for credits.)

which a proximal domain occupant was in residence, including occupancy by $Q^{\bullet -}$. These characteristics allow us to suggest an escapement mechanism for gating that might be likened to regulation in a clock. The "pendulum" of the mobile domain of ISP, would be linked to a "ratchet" provided by the -PEWY- see-saw and associated conformational changes at the trapdoor [51]. The effect would be to allow access for ISP to the Q_o-site occupant to favor binding, only when the proximal domain is vacated after oxidation of $Q^{\bullet -}$ by heme b_L, and when Q or QH_2 are present as inoffensive binding partners to ISPH or ISP_{ox}, respectively, in the distal domain.

5.3. Gating in the second electron transfer

Several groups have demonstrated through kinetic modeling that when a single rate constant (k_{2d} ~10^6 s^{-1}, that for electron transfer from the distal domain given by distance) is used, the reactions become uncoupled; high rates for bypass processes are predicted for the antimycin-inhibited chain [86,87,91], or the chain blocked by disabling the binding of heme b_H [91], or backed-up by the proton gradient [42]. This is because, as pointed out by Osyczka et al. [43], if a single rate constant defined by distance is used, the same distance applies to bypass processes, some of which would have strongly favorable driving forces, so that bypass rates modeled on this basis would be comparable to those for normal forward chemistry. However, the bypass rates observed experimentally are much lower, even in strains with mutations at E295 [78], where a strong decoupling might also be expected. The spatial separation of distal and proximal domains, the likelihood that $Q^{\bullet -}$ must diffuse through this distance to realize the rapid rate required, and separation of the second electron transfer into partial processes associated with this topology, open several possibilities for control and/or gating to provide a way out of this paradox. The value for k_{2d} ~10^3 s^{-1} demonstrated in our recent work [78] explains the phenomenon in the E295 mutants in terms of a limit on both forward and reverse processes. In the strains with bulky sidechains, the SQ_o would be constrained to the domain distal from heme b_L, and all rate constants involving interaction with heme b_L would reflect that distance. Loss of catalysis of proton exit would apply to both forward and reverse processes, and would further limit both. Since the forward rate constant is lowered by 10^3-fold from the value given by distance, and equilibrium constants are conserved, backward rate constants will be lowered by a similar ratio, thus limiting

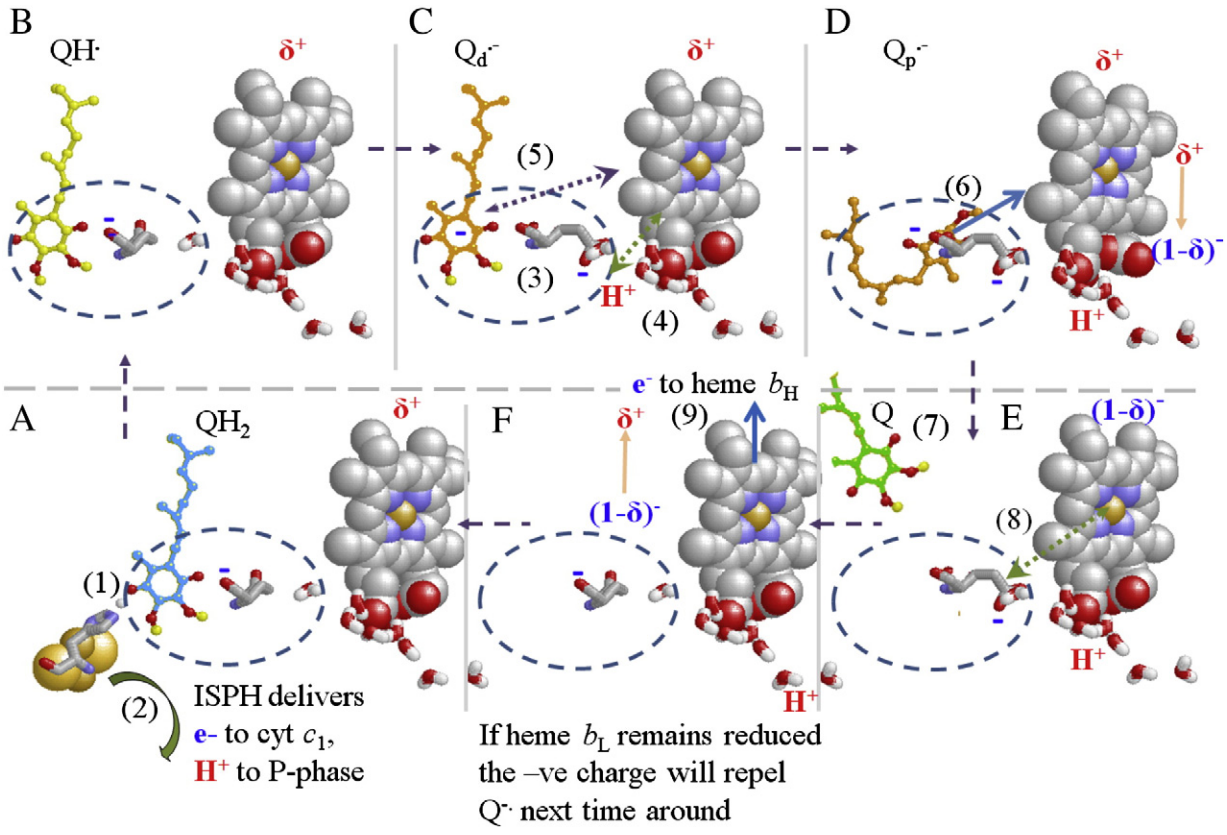

Fig. 7. Scheme to show possible mechanistic features of the Q_o-site ballet (from [78]). The first electron transfer is encapsulated on frame A, though details of partial processes and of the escapement gating mechanism are omitted. A possible scenario for the coulombic choreography of the second electron transfer and the exit of the associated proton is shown in frames B through F. In order to minimize production of ROS (perhaps the black swan of this ballet), the first electron transfer is strongly endergonic, and the second electron transfer has to remove the intermediate SQ_o rapidly, in competition with the backward rate constant for the first step [46,48]. A. Before the 1st electron transfer, ES_1 forms in the distal volume of the Q_o-site, stabilized by a strong H-bond to His-161 of ISP_{ox}. E295 may H-bond weakly to QH_2. Heme b_L is in the oxidized form (with local field of δ^+ charge). An electron and H^+ are delivered to ISP_{ox} to form ISPH (1). Immediately after the 1st electron transfer, the ISPH rotates away (2) to deliver its electron to cyt c_1 and release the H^+ to the P-phase. B. This leaves the neutral SQ (QH•), H-bonded to E295 carboxylate in ES_2. Heme b_L is still oxidized, and available as acceptor for the electron from QH• (or $Q^{\bullet -}$), but the low occupancy, and low value for k_{2d} (~10^3 s^{-1}) mean the rate is slow. C. The H^+ is transferred to the E295 carboxylate, to form the SQ anion ($Q^{\bullet -}$), and E295 (3), now in carboxylic form, rotates to open up the proximal volume. The sidechain makes an H-bond to the water chain leading to the P-side aqueous phase. The δ^+ field around heme b_L lowers the pK, allowing the release of the H^+ (4), which transfers down the water chain, leaving E295 in the carboxylate form. The δ^+ field also attracts $Q^{\bullet -}$ (5), which migrates closer to heme b_L, increasing the rate constant (k_{2p} ~10^9 s^{-1}). D. The electron from $Q^{\bullet -}$ transfers rapidly to heme b_L (6), and the quinone is free to migrate back to the distal volume, and exit the site (7). Reduction of heme b_L changes the charge by 1, and the field changes transiently to $(1-\delta)^-$. E. The field is felt by the carboxylate of E295 (8), and the coulombic force flips it back to its initial position. F. If heme b_H is oxidized, the electron is transferred (9), and the field associated with heme b_L returns to its initial δ^+ charge. The site is now vacant, and available to accept a QH_2 for the next turnover. If heme b_L remains reduced (after the second turnover if antimycin is present), the $(1-\delta)^-$ field serves to repel the $Q^{\bullet -}$ formed after the next cycle (reactions (1)–(3) representing a partial third turnover).

rates involving ferroheme b_L as donor. An explanation for control of the bifurcated reaction might therefore be sought through constraints that restrict SQ to the distal domain, and/or inhibit proton processing. We have previously suggested such a mechanism operating through coulombic repulsion [10], and discuss other scenarios in Section 5.5.

5.4. Electrostatic profiles in the bc_1 complex

Central to any discussion of control through coulombic interaction is the electrostatic profile along the reaction coordinate. For a complex mechanism like the Q-cycle, the overall process must accommodate a substantial volume. The case is somewhat simplified if we restrict consideration to the second electron transfer. We have used the model set up for MD simulation in a preliminary exploration of local electrostatics through PME analysis in VMD to generate profiles of the *Rb. sphaeroides* bc_1 complex, taking an average from 150 equally spaced frames from a 10 ns simulation in NAMD. Fig. 6 shows two isosurface representations for contours in the negative (red) and positive (blue) ranges, selected so as to show well-defined volumes. In the simulation, the hemes were all in the reduced state. As a consequence, differences in potential reflect contributions from the protein. Even with this relatively naïve approach, several features are striking. Factors that might modulate kinetic pathways and redox potentials of heme groups are particularly obvious. The central dumbbell-shaped negative volume encloses the hemes b_L, and the protein between them forming the putative pathway for electron transfer. The residues in the direct path all have polar sidechains but they are surrounded by a cylinder of nonpolar residues shielding them from the solvent and the rest of the protein. This negatively charged volume would have the effect of lowering the probability for electron transfer into the volume, and might be an important factor in limiting electron transfer through this interface. In contrast, the path between b_L and b_H is more neutral, so would not disfavor electron transfer. The smaller volumes enclosed by the profiles around the hemes b_H suggest lower charge densities. This differential charge density would account at least in part for the difference in redox potentials between the two hemes. Similarly, the strongly positive volumes around the heme c_1 would account in part for their high redox potential. The [Fe_2S_2] cluster of ISP shows no strong field associated with the volume. However, conserved arginine residues in the extrinsic domain, well separated from the cluster, show a significant positive field. This is likely static, but could perhaps be invoked in a coulombic control associated with a changing field around heme c_1. One other feature worth noting is an aspartate from cyt *b* (Asp-373 in trans-membrane helix G of each monomer) projecting into the membrane in the middle of the insulating phase. This feature is semi-conserved (either Asp or Asn) across mitochondrial and α-proteobacteria sequences. There seems no obvious role for such a local field, since there are no compensating groups in the three main subunits of the bc_1 complex, and the missing subunit IV has no appropriately charged positive group in the putative membrane domain. But perhaps the site is involved in specific interaction with some other structure in the membrane.

5.5. Scenarios for mechanism

The scheme of Fig. 7 (taken from [78]) shows a speculative cycle of partial processes for the Q_o-site that includes some coulombic interactions that might serve a control function. Several dancers join a ballet of dynamic changes in the protein. $Q^{\bullet -}$, the E295 carboxylate, heme b_L and its propionates, the proton and electron when free of carriers, are all coulombic players generated at different stages in the dance. Since the charges separate on transfer of H^+ to E295, coulombic interactions will come into play, superimposed in existing static fields. In the scheme, we assume that the ferriheme b_L initially carries a partial positive charge, changing to a partial negative charge on reduction. This would allow two coulombic effects: (i) an attractive force favoring movement of $Q^{\bullet -}$ in the site towards the heme, and (ii) after reduction, a repulsive force constraining $Q^{\bullet -}$ to the distal domain so as to favor only the slow rate constants appropriate to that domain. These would pertain under conditions in which bypass by reduction of SQ_o by ferroheme b_L might occur. Additional coulombic interactions seem feasible. Since the rotational displacement of E295 in the carboxylic state has to precede the movement of $Q^{\bullet -}$, the partial positive charge in ferriheme b_L would stabilize the carboxylate and favor dissociation to release the proton, and the partial negative charge after electron transfer would favor movement of the E295 carboxylate back to the distal configuration as soon as Q vacates the site.

Although the scheme of Fig. 7 is speculative, the principles inspiring it are quite natural, and it is likely that some such a ballet steers the reaction. Because these processes are not readily accessible to direct study, an approach through computational simulation seems likely to be rewarding, and our preliminary efforts here represent a step in this direction.

Acknowledgements

ARC thanks NIH for the support through grant RO1 GM035438, RB and SH thank Dr. Sergei Dikanov for the support under NIH RO1 GM062954, KS and CH acknowledge support through NIH PHS 9 P41 GM104601 and NSF PHY0822613, and CW thanks the Center for Biophysics and Computational Biology for the support through a Research Assistantship for Summer 2012.

References

[1] P. Mitchell, Possible molecular mechanisms of the protonmotive function of cytochrome systems, J. Theor. Biol. 62 (1976) 327–367.
[2] A.R. Crofts, S.W. Meinhardt, K.R. Jones, M. Snozzi, The role of the quinone pool in the cyclic electron-transfer chain of *Rhodopseudomonas sphaeroides*: a modified Q-cycle mechanism, Biochim. Biophys. Acta 723 (1983) 202–218.
[3] A.R. Crofts, The Q-cycle, — a personal perspective, Photosynth. Res. 80 (2004) 223–243.
[4] A.R. Crofts, V.P. Shinkarev, D.R.J. Kolling, S. Hong, The modified Q-cycle explains the apparent mismatch between the kinetics of reduction of cytochromes c_1 and b_H in the bc_1 complex, J. Biol. Chem. 278 (2003) 36191–36201.
[5] P.B. Garland, R.A. Clegg, D. Boxer, J.A. Downie, B.A. Haddock, Proton-translocating nitrate reductase of *Escherichia coli*, in: E. Quagliariello, S. Papa, F. Palmieri, E.C. Slater, N. Siliprandi (Eds.), Electron Transfer Chains and Oxidative Phosphorylation, North-Holland Publishing Co., Amsterdam, The Netherlands, 1975, pp. 351–358.
[6] Z. Zhang, L.-S. Huang, V.M. Shulmeister, Y.-I. Chi, K.-K. Kim, L.-W. Hung, A.R. Crofts, E.A. Berry, S.-H. Kim, Electron transfer by domain movement in cytochrome bc_1, Nature (Lond.) 392 (1998) 677–684.
[7] A.R. Crofts, The cytochrome bc_1 complex — function in the context of structure, Annu. Rev. Physiol., 2004, pp. 689–733.
[8] A. Osyczka, C.C. Moser, F. Daldal, P.L. Dutton, Reversible redox energy coupling in electron transfer chains, Nature 427 (2004) 607–612.
[9] A.R. Crofts, J.T. Holland, D. Victoria, D.R. Kolling, S.A. Dikanov, R. Gilbreth, S. Lhee, R. Kuras, M.G. Kuras, The Q-cycle reviewed: how well does a monomeric mechanism of the bc_1 complex account for the function of a dimeric complex? Biochim. Biophys. Acta 1777 (2008) 1001–1019.
[10] A.R. Crofts, S. Lhee, S.B. Crofts, J. Cheng, S. Rose, Proton pumping in the bc_1 complex: a new gating mechanism that prevents short circuits, Biochim. Biophys. Acta 1757 (2006) 1019–1034.
[11] D.J. Kolling, J.S. Brunzelle, S. Lhee, A.R. Crofts, S.K. Nair, Atomic resolution structures of Rieske iron–sulfur protein: role of hydrogen bonds in tuning the redox potential of iron–sulfur clusters, Structure 15 (2007) 29–38.
[12] E.A. Berry, D.-W. Lee, L.-S. Huang, F. Daldal, Structural and mutational studies of the cytochrome bc_1 complex, in: C.N. Hunter, F. Daldal, M.C. Thurnauer, J.T. Beatty (Eds.), The Purple Phototrophic Bacteria, Springer, Dordrecht, The Netherlands, 2009.
[13] S. Lhee, D.R. Kolling, S.K. Nair, S.A. Dikanov, A.R. Crofts, Modifications of protein environment of the [2Fe–2S] cluster of the bc_1 complex: effects on the biophysical properties of the Rieske iron–sulfur protein and on the kinetics of the complex, J. Biol. Chem. 285 (2010) 9233–9248.
[14] M. Castellani, R. Covian, T. Kleinschroth, O. Anderka, B. Ludwig, B.L. Trumpower, Direct demonstration of half-of-the-sites reactivity in the dimeric cytochrome bc_1 complex, J. Biol. Chem. 285 (2010) 502–510.
[15] R. Covián, B.L. Trumpower, Rapid electron transfer between monomers when the cytochrome bc_1 complex dimer is reduced through center N, J. Biol. Chem. 280 (2005) 22732–22740.
[16] P. Lanciano, D.-W. Lee, H. Yang, E. Darrouzet, F. Daldal, Intermonomer electron transfer between the low-potential *b* hemes of cytochrome bc_1, Biochemistry 50 (2011) 1651–1663.

[17] A.Y. Mulkidjanian, Ubiquinol oxidation in the cytochrome b_1 complex: reaction mechanism and prevention of short-circuiting, Biochim. Biophys. Acta 1709 (2005) 5–34.
[18] A.Y. Mulkidjanian, Proton translocation by the cytochrome bc1 complexes of phototrophic bacteria: introducing the activated Q-cycle, Photochem. Photobiol. Sci. 6 (2007) 19–34.
[19] M. Świerczek, E. Cieluch, M. Sarewicz, A. Borek, C.C. Moser, P.L. Dutton, A. Osyczka, An electronic bus bar lies in the core of cytochrome bc_1, Science 329 (2010) 451–454.
[20] B.L. Trumpower, A concerted, alternating sites mechanism of ubiquinol oxidation by the dimeric cytochrome bc_1 complex, Biochim. Biophys. Acta 1555 (2002) 166–173.
[21] J.W. Cooley, T. Ohnishi, F. Daldal, Binding dynamics at the quinone reduction (Q_i) site influence the equilibrium interactions of the iron sulfur protein and hydroquinone oxidation (Q_o) site of the cytochrome bc_1 complex, Biochemistry 44 (2005) 10520–10532.
[22] X. Gong, L. Yu, D. Xia, C.-A. Yu, Evidence for electron equilibrium between the two hemes b_L in the dimeric cytochrome bc_1 complex, J. Biol. Chem. 280 (2005) 9251–9257.
[23] C.-A. Yu, X. Wen, K. Xiao, D. Xia, L. Yu, Inter- and intra-molecular electron transfer in the cytochrome bc_1 complex, Biochim. Biophys. Acta 1555 (2002) 65–70.
[24] V.P. Shinkarev, C.A. Wraight, Intermonomer electron transfer in the bc_1 complex dimer is controlled by the energized state and by impaired electron transfer between low and high potential hemes, FEBS Lett. 581 (2007) 1535–1541.
[25] A.R. Crofts, The mechanism of ubiquinol:cytochrome c oxidoreductases of mitochondria and of *Rhodopseudomonas sphaeroides*, in: A.N. Martonosi (Ed.), The Enzymes of Biological Membranes, Plenum Publ. Corp., New York., 1985, pp. 347–382.
[26] A.R. Crofts, S.W. Meinhardt, A Q-cycle mechanism for the cyclic electron transfer chain of *Rps. sphaeroides*, Biochem. Soc. Trans. 10 (1982) 201–203.
[27] E.G. Glaser, A.R. Crofts, A new electrogenic step in the ubiquinol: cytochrome c2 oxidoreductase complex of *Rhodopseudomonas sphaeroides*, Biochim. Biophys. Acta Bioenerg. 766 (1984) 322–333.
[28] S.W. Meinhardt, A.R. Crofts, Kinetic and thermodynamic resolution of cytochrome c_1 and cytochrome c_2 from *Rps. sphaeroides*, FEBS Lett. 149 (1982) 223–227.
[29] S.W. Meinhardt, A.R. Crofts, The role of cytochrome b_{566} in the electron transfer chain of *Rps. sphaeroides*, Biochim. Biophys. Acta 723 (1983) 219–230.
[30] M. Czapla, A. Borek, M. Sarewicz, A. Osyczka, Enzymatic activities of isolated cytochrome bc_1-like complexes containing fused cytochrome *b* subunits with asymmetrically inactivated segments of electron transfer chains, Biochemistry 51 (2012) 829–835.
[31] M. Czapla, A. Borek, M. Sarewicz, A. Osyczka, Fusing two cytochromes *b* of *Rhodobacter capsulatus* cytochrome bc_1 using various linkers defines a set of protein templates for asymmetric mutagenesis, Protein Eng. Des. Sel. 25 (2012) 15–25.
[32] B. Khalfaoui-Hassani, P. Lanciano, D.W. Lee, E. Darrouzet, F. Daldal, Recent advances in cytochrome bc_1: inter monomer electronic communication? FEBS Lett. 586 (2012) 617–621.
[33] S. Hong, D. Victoria, A.R. Crofts, Inter-monomer electron transfer is too slow to compete with monomeric turnover in bc_1 complex, Biochim. Biophys. Acta 1817 (2012) 1053–1062.
[34] A.W. Rutherford, A. Osyczka, F. Rappaport, Back-reactions, short-circuits, leaks and other energy wasteful reactions in biological electron transfer: redox tuning to survive life in O_2, FEBS Lett. 586 (2012) 603–616.
[35] D. Noy, C.C. Moser, P.L. Dutton, Darwin at the molecular scale: selection and variance in electron tunnelling proteins including cytochrome c oxidase, Biochim. Biophys. Acta 1757 (2006) 90–106.
[36] K.B. Beckman, B.N. Ames, The free radical theory of aging matures, Physiol. Rev. 78 (1998) 547–581.
[37] D. Harman, Aging: a theory based on free radical and radiation chemistry, J. Gerontology 11 (1956) 298–300.
[38] D. Harman, Free radical theory of aging, in: I. Emerit, B. Chance (Eds.), Free Radicals and Aging, Birkhauser Verlag, Basel., 1992
[39] S. Raha, B.H. Robinson, Mitochondria, oxygen free radicals, and apoptosis, Am. J. Med. Genetics 106 (2001) 62–70.
[40] F. Muller, A.R. Crofts, D.M. Kramer, Multiple Q-cycle bypass reactions at the Q_o-site of the cytochrome bc_1 complex, Biochemistry 41 (2002) 7866–7874.
[41] A. Boveris, B. Chance, The mitochondrial generation of hydrogen peroxide. General properties and effect of hyperbaric oxygen, Biochem. J. 134 (1973) 707–716.
[42] H. Rottenberg, R. Covian, B.L. Trumpower, Membrane potential greatly enhances superoxide generation by the cytochrome bc1 complex reconstituted into phospholipid vesicles, J. Biol. Chem. 284 (2009) 19203–19210.
[43] A. Osyczka, C.C. Moser, P.L. Dutton, Fixing the Q-cycle, Trends Biochem. Sci. 30 (2005) 176–182.
[44] A.R. Crofts, Proton-coupled electron transfer at the Q_o-site of the bc_1 complex controls the rate of ubihydroquinone oxidation, Biochim. Biophys. Acta 1655 (2004) 77–92.
[45] A.R. Crofts, Z. Wang, How rapid are the internal reactions of the ubiquinol:cytochrome c_2 oxidoreductase? Photosynth. Res. 22 (1989) 69–87.
[46] S. Junemann, P. Heathcote, P.R. Rich, On the mechanism of quinol oxidation in the bc_1 complex, J. Biol. Chem. 273 (1998) 21603–21607.
[47] S.J. Hong, N. Ugulava, M. Guergova-Kuras, A.R. Crofts, The energy landscape for ubihydroquinone oxidation at the Q_o-site of the bc_1 complex in *Rhodobacter sphaeroides*, J. Biol. Chem. 274 (1999) 33931–33944.
[48] P.R. Rich, The quinone chemistry of *bc* complexes, Biochim. Biophys. Acta 1658 (2004) 165–171.
[49] A.R. Crofts, B. Barquera, R.B. Gennis, R. Kuras, M. Guergova-Kuras, E.A. Berry, Mechanism of ubiquinol oxidation by the bc_1 complex: the different domains of the quinol binding pocket, and their role in mechanism, and the binding of inhibitors, Biochemistry 38 (1999) 15807–15826.
[50] A.R. Crofts, M. Guergova-Kuras, L.-S. Huang, R. Kuras, Z. Zhang, E.A. Berry, The mechanism of ubiquinol oxidation by the bc_1 complex: the role of the iron sulfur protein, and its mobility, Biochemistry 38 (1999) 15791–15806.
[51] A.R. Crofts, M. Guergova-Kuras, R. Kuras, N. Ugulava, J. Li, S. Hong, Proton-coupled electron transfer at the Q_o-site: what type of mechanism can account for the high activation barrier? Biochim. Biophys. Acta 1459 (2000) 456–466.
[52] A.R. Crofts, M. Guergova-Kuras, N. Ugulava, R. Kuras, S. Hong, Proton processing at the Q_o-site of the bc_1 complex of *Rhodobacter sphaeroides*, Proc. XIIth Congress of Photosynthesis Research, Brisbane, Australia, 2002, p. 6.
[53] A.R. Crofts, S. Hong, Z. Zhang, E.A. Berry, Physicochemical aspects of the movement of the Rieske iron sulfur protein during quinol oxidation by the bc_1 complex, Biochemistry 38 (1999) 15827–15839.
[54] A.R. Crofts, S.J. Hong, N. Ugulava, B. Barquera, R. Gennis, M. Guergova-Kuras, E.A. Berry, Pathways for proton release during ubihydroquinone oxidation by the bc_1 complex, Proc. Natl. Acad. Sci. U. S. A. 96 (1999) 10021–10026.
[55] J.L. Cape, M.K. Bowman, D.M. Kramer, A semiquinone intermediate generated at the Q_o site of the cytochrome bc_1 complex: importance for the Q-cycle and superoxide production, Proc. Natl. Acad. Sci. U. S. A. 104 (2007) 7887–7892.
[56] R. Covián, B.L. Trumpower, The rate-limiting step in the cytochrome bc_1 complex is not changed by inhibition of cytochrome b-dependent deprotonation: implications for the mechanism of ubiquinol oxidation at center P of the bc_1 complex, J. Biol. Chem. 284 (2009) 14359–14367.
[57] H. Zhang, A. Osyczka, P.L. Dutton, C.C. Moser, Exposing the complex III Q_o semiquinone radical, Biochim. Biophys. Acta 1767 (2007) 883–887.
[58] J.A. Roberts, J.P. Kirby, S.T. Wall, D.G. Nocera, Electron transfer within ruthenium(II) polypyridyl-(salt bridge)-dimethylaniline acceptor-donor complexes, Inorg. Chim. Acta 263 (1997) 395–405.
[59] M. Guergova-Kuras, R. Kuras, N. Ugulava, I. Hadad, A.R. Crofts, Specific mutagenesis of the Rieske iron sulfur protein in *Rhodobacter sphaeroides* shows that both thermodynamic gradient and the pK of the oxidized form determine the rate of quinol oxidation by the bc_1 complex, Biochemistry 39 (2000) 7436–7444.
[60] S. Lhee, D.R. Kolling, S.K. Nair, S.A. Dikanov, A.R. Crofts, Modifications of protein environment of the [2Fe–2S] cluster of the bc_1 complex: effects on the biophysical properties of the Rieske iron–sulfur protein and on the kinetics of the complex, J. Biol. Chem. 285 (2009) 9233–9248.
[61] M. Snozzi, A.R. Crofts, Electron transport in chromatophores from *Rhodopseudomonas sphaeroides* GA fused with liposomes, Biochim. Biophys. Acta Bioenerg. 766 (1984) 451–463.
[62] Y. Zu, M.M.-J. Couture, D.R.J. Kolling, A.R. Crofts, L.D. Eltis, J.A. Fee, J. Hirst, The reduction potentials of Rieske clusters: the importance of the coupling between oxidation state and histidine protonation state, Biochemistry 42 (2003) 12400–12408.
[63] U. Brandt, J.G. Okun, Role of deprotonation events in ubihydroquinone: cytochrome c oxidoreductase from bovine heart and yeast mitochondria, Biochemistry 36 (1997) 11234–11240.
[64] E. Denke, T. Merbitzzahradnik, O.M. Hatzfeld, C.H. Snyder, T.A. Link, B.L. Trumpower, Alteration of the midpoint potential of the Rieske iron–sulfur protein by changes of amino acids forming H-bonds to the iron–sulfur cluster, J. Biol. Chem. 273 (1998) 9085–9093.
[65] T. Schröter, O.M. Hatzfeld, S. Gemeinhardt, M. Korn, T. Friedrich, B. Ludwig, T. Link, Mutational analysis of residues forming hydrogen bonds in the Rieske [2Fe2S] cluster of the cytochrome bc_1 complex of *Paracoccus denitrificans*, Eur. J. Biochem. 255 (1998) 100–106.
[66] S.A. Dikanov, D.R.J. Kolling, B. Endeward, R.I. Samoilova, T.F. Prisner, S.K. Nair, A.R. Crofts, Identification of hydrogen bonds to the rieske cluster through the weakly coupled nitrogens detected by electron spin echo envelope modulation spectroscopy, J. Biol. Chem. 281 (2006) 27416–27425.
[67] D.R. Kolling, R.I. Samoilova, A.A. Shubin, A.R. Crofts, S.A. Dikanov, Proton environment of reduced Rieske iron–sulfur cluster probed by two-dimensional ESEEM spectroscopy, J. Phys. Chem. A 113 (2009) 653–667.
[68] R.I. Samoilova, D. Kolling, T. Uzawa, T. Iwasaki, A.R. Crofts, S.A. Dikanov, The interaction of the Rieske iron sulfur protein with occupants of the Q_o-site of the bc_1 complex, probed by 1D and 2D electron spin echo envelope modulation, J. Biol. Chem. 277 (2002) 4605–4608.
[69] I.-J. Lin, Y. Chen, J.A. Fee, J. Song, W.M. Westler, J.L. Markley, Rieske protein from *Thermus thermophilus*: ^{15}N NMR titration study demonstrates the role of iron-ligated histidines in the pH dependence of the reduction potential, J. Am. Chem. Soc. 128 (2006) 10672–10673.
[70] K.-L. Hsueh, W.M. Westler, J.L. Markley, NMR investigations of the Rieske protein from *Thermus thermophilus* support a coupled proton and electron transfer mechanism, J. Am. Chem. Soc. 132 (2010) 7908–7918.
[71] S. Izrailev, A.R. Crofts, E.A. Berry, K. Schulten, Steered molecular dynamics simulation of the Rieske subunit motion in the cytochrome bc_1 complex, Biophys. J. 77 (1999) 1753–1768.
[72] L. Esser, M. Elberry, F. Zhou, C.-A. Yu, L. Yu, D. Xia, Inhibitor complexed structures of the cytochrome bc_1 complex from the photosynthetic bacterium *Rhodobacter sphaeroides*, J. Biol. Chem. 283 (2008) 2846–2857.
[73] C. Hunte, J. Koepke, C. Lange, T. Roßmanith, H. Michel, Structure at 2.3 Å resolution of the cytochrome bc_1 complex from the yeast *Saccharomyces cerevisiae* co-crystallized with an antibody F_v fragment, Structure 8 (2000) 669–684.
[74] A. Osyczka, H. Zhang, C. Mathé, P.R. Rich, C.C. Moser, P.L. Dutton, Role of the PEWY glutamate in hydroquinone-quinone oxidation–reduction catalysis in the Q_o site of cytochrome bc_1, Biochemistry 45 (2006) 10492–10503.

[75] T. Wenz, R. Covian, P. Hellwig, F. MacMillan, B. Meunier, B.L. Trumpower, C. Hunte, Mutational analysis of cytochrome b at the ubiquinol oxidation site of yeast complex III, J. Biol. Chem. 282 (2006) 3977–3988.
[76] T. Wenz, P. Hellwig, F. MacMillan, B. Meunier, C. Hunte, Probing the role of E272 in quinol oxidation of mitochondrial complex III, Biochemistry 45 (2006) 9042–9052.
[77] N. Seddiki, B. Meunier, D. Lemesle-Meunier, G. Brasseur, Is cytochrome b glutamic acid 272 a quinol binding residue in the bc_1 complex of *Saccharomyces cerevisiae*? Biochemistry 47 (2008) 2357–2368.
[78] D. Victoria, R. Burton, A.R. Crofts, Role of the -PEWY- glutamate in catalysis at the Q_o-site of the cyt bc_1 complex, Biochim. Biophys. Acta (2012), http://dx.doi.org/10.1016/j.bbabio.2012.10.012.
[79] G. Engstrom, K. Xiao, C.-A. Yu, L. Yu, B. Durham, F. Millett, Photoinduced electron transfer between the Rieske iron–sulfur protein and cytochrome c_1 in the *Rhodobacter sphaeroides* cytochrome bc_1 complex: effects of pH, temperature, and driving force, J. Biol. Chem. 277 (2002) 31072–31078.
[80] J. Zhu, T. Egawa, S.R. Yeh, L. Yu, C.-A. Yu, Simultaneous reduction of iron–sulfur protein and cytochrome b_L during ubiquinol oxidation in cytochrome bc_1 complex, Proc. Natl. Acad. Sci. U. S. A. 104 (2007) 4864–4869.
[81] S. de Vries, S.P.J. Albracht, J.A. Berden, E.C. Slater, A new species of bound ubisemiquinone anion in QH_2: cytochrome *c* oxidoreductase, J. Biol. Chem. 256 (1981) 11996–11998.
[82] K.M. Andrews, A.R. Crofts, R.B. Gennis, Large scale purification and characterization of a highly active four-subunit cytochrome bc_1 complex from *Rb. sphaeroides*, Biochemistry 29 (1990) 2645–2651.
[83] T.A. Link, Two pK values of the oxidised 'Rieske' [2Fe–2S] cluster observed by CD spectroscopy, Biochim. Biophys. Acta 1185 (1994) 81–84.
[84] P. Kuzmic, Program DYNAFIT for the analysis of enzyme kinetic data: application to HIV proteinase, Anal. Biochem. 237 (1996) 260–273.
[85] N. Kim, M.O. Ripple, R. Springett, Measurement of the mitochondrial membrane potential and pH gradient from the redox poise of the hemes of the bc_1 complex, Biophys. J. 102 (2012) 1194–1203.
[86] S. Ransac, J.-P. Mazat, How does antimycin inhibit the bc_1 complex? A part-time twin, Biochim. Biophys. Acta 1797 (2010) 1849–1857.
[87] S. Ransac, N. Parisey, J.-P. Mazat, The loneliness of the electrons in the bc_1 complex, Biochim. Biophys. Acta 1777 (2008) 1053–1059.
[88] M.F. Blackwell, J. Whitmarsh, Effect of integral membrane proteins on the lateral mobility of plastoquinone in phosphatidylcholine proteoliposomes, Biophys. J. 58 (1990) 1259–1271.
[89] K. Rajarathnam, J. Hochman, M. Schindler, S. Ferguson-Miller, Synthesis, location, and lateral mobility of fluorescently labeled ubiquinone-10 in mitochondrial and artificial membranes, Biochemistry 28 (1989) 3168–3176.
[90] C.C. Moser, C.C. Page, X.X. Chen, P.L. Dutton, Biological electron tunnelling through protein media, J. Biol. Inorg. Chem. 2 (1997) 393–398.
[91] C.C. Moser, T.A. Farid, S.E. Chobot, P.L. Dutton, Electron tunnelling chains of mitochondria, Biochim. Biophys. Acta 1757 (2006) 1096–1109.
[92] C.C. Moser, J.M. Keske, K. Warncke, R.S. Farid, P.L. Dutton, Nature of biological electron transfer, Nature 355 (1992) 796–802.
[93] J.J. Hopfield, Electron transfer between biological molecules by thermally activated tunneling, Proc. Natl. Acad. Sci. U. S. A. 71 (1974) 3640–3644.
[94] D. DeVault, Quantum mechanical tunnelling in biological systems, Q. Rev. Biophys. 13 (1980) 387–564.
[95] C.C. Moser, C.C. Page, R. Farid, P.L. Dutton, Biological electron transfer, J. Bioenerg. Biomembr. 27 (1995) 263–274.
[96] A.R. Crofts, S. Rose, Marcus treatment of endergonic reactions: a commentary, Biochim. Biophys. Acta 1767 (2007) 1228–1232.
[97] C.C. Page, C.C. Moser, X.X. Chen, P.L. Dutton, Natural engineering principles of electron tunnelling in biological oxidation–reduction, Nature 402 (1999) 47–52.
[98] R.A. Marcus, On the theory of electron-transfer reactions. VI. Unified treatment of homogeneous and electrode reactions, J. Chem. Phys. 43 (1965) 679–701.
[99] A. Warshel, A. Papazyan, Electrostatic effects in macromolecules: fundamental concepts and practical modeling, Curr. Opin. Struct. Biol. 8 (1998) 211–217.
[100] A. Warshel, W.W. Parson, Dynamics of biochemical and biophysical reactions: insight from computer simulations, Q. Rev. Biophys. 34 (2001) 563–679.
[101] W.W. Parson, A. Warshel, Dependence of photosynthetic electron-transfer kinetics on temperature and energy in a density-matrix model, J. Phys. Chem. B 108 (2004) 10474–10483.
[102] H. Wang, S. Lin, E. Katilius, C. Laser, J.P. Allen, J.C. Williams, N.W. Woodbury, Unusual temperature dependence of photosynthetic electron transfer due to protein dynamics, J. Phys. Chem. B 113 (2009) 818–824.
[103] D.N. LeBard, V. Kapko, D.V. Matyushov, Energetics and kinetics of primary charge separation in bacterial photosynthesis, J. Phys. Chem. B 112 (2008) 10322–10342.
[104] L.I. Krishtalik, The medium reorganization energy for the charge transfer reactions in proteins, Biochim. Biophys. Acta 1807 (2011) 1444–1456.
[105] M. Wikström, M.I. Verkhovskya, G. Hummer, Water-gated mechanism of proton translocation by cytochrome c oxidase, Biochim. Biophys. Acta 1604 (2003) 61–65.
[106] A.S. Saribas, H. Ding, P.L. Dutton, F. Daldal, Tyrosine 147 of cytochrome *b* is required for efficient electron transfer at the ubihydroquinone oxidase site (Q_o) of the cytochrome bc_1 complex, Biochemistry 34 (1995) 16004–16012.
[107] L. Esser, X. Gong, S. Yang, L. Yu, C.-A. Yu, D. Xia, Surface-modulated motion switch: capture and release of iron–sulfur protein in the cytochrome bc_1 complex, Proc. Natl. Acad. Sci. U. S. A. 103 (2006) 13045–13050.
[108] D.-W. Lee, N. Selamoglu, P. Lanciano, J.W. Cooley, I. Forquer, D.M. Kramer, F. Daldal, Loss of a conserved tyrosine residue of cytochrome *b* induces reactive oxygen species production by cytochrome bc_1, J. Biol. Chem. 286 (2011) 18139–18148.
[109] E.A. Berry, L.-S. Huang, Conformationally linked interaction in the cytochrome bc_1 complex between inhibitors of the Q_o site and the Rieske iron–sulfur protein, Biochim. Biophys. Acta 1807 (2011) 1349–1363.
[110] F. Wibrand, K. Ravn, M. Schwartz, T. Rosenberg, N. Horn, J. Vissing, Multisystem disorder associated with a missense mutation in the mitochondrial cytochrome *b* gene, Ann. Neurol. 50 (2001) 540–543.
[111] I.K. Srivastava, J.M. Morrisey, E. Darrouzet, F. Daldal, A.B. Vaidya, Resistance mutations reveal the atovaquone-binding domain of cytochrome b in malaria parasites, Mol. Microbiol. 33 (1999) 704–711.
[112] J.R. Bowyer, A.R. Crofts, On the mechanism of photosynthetic electron transfer in *Rps. capsulata* and *Rps. sphaeroides*, Biochim. Biophys. Acta 636 (1981) 218–233.